

1 Calcification response of planktic foraminifera to environmental change in the
2 Western Mediterranean Sea during the industrial era

3

4 Thibault M. Béjard^{1*}, Andrés S. Rigual-Hernández¹, José A. Flores¹, Javier P.
5 Tarruella¹, Xavier Durrieu de Madron², Isabel Cacho³, Neghar Haghypour⁴, Aidan
6 Hunter⁵, Francisco J. Sierro¹

7

8 1. Area de Paleontología, Departamento de Geología, Universidad de Salamanca,
9 37008 Salamanca, Spain

10 2. Université de Perpignan Via Domitia, CNRS, CEFREM, Perpignan, France

11 3. GRC Geociències Marines, Departament de Dinàmica de la Terra i de l'Oceà,
12 Facultat de Ciències de la Terra, Universitat de Barcelona, Barcelona, Spain

13 4. Earth Sciences Department, ETH Zurich, Zurich, 8092, Switzerland

14 5. British Antarctic Survey, Natural Environment Research Council, Cambridge,
15 United Kingdom

16 Tom parker

17 *Corresponding autor. E-mail address: thibault.bejard@usal.es.

18 Abstract

19

20 The Mediterranean Sea sustains a rich and fragile ecosystem currently threatened
21 by multiple anthropogenic impacts that include, among others, warming, pollution
22 and changes in seawater carbonate speciation associated to increasing uptake of
23 atmospheric CO₂. This environmental change represents a major risk for marine
24 calcifiers such as planktonic foraminifera, key components of pelagic Mediterranean
25 ecosystems and major exporters of calcium carbonate to the sea floor, thereby
26 playing a major role in the marine carbon cycle. In this study, we investigate the
27 response of planktic foraminifera calcification in the northwestern Mediterranean
28 Sea on different time scales across the industrial era. This study is based on data
29 from a 12-year-long sediment trap record retrieved in the in the Gulf of Lions and
30 seabed sediment samples from the Gulf of Lions and the promontory of Menorca.
31 Three different planktic foraminifera species were selected based on their different
32 ecology and abundance: *Globigerina bulloides*, *Neogloboquadrina incompta*, and
33 *Globorotalia truncatulinoides*. A total of 273 samples were weighted in both sediment
34 trap and seabed samples.

35 The results of our study suggest substantial different seasonal calcification patterns
36 across species: *G. bulloides* shows a slight calcification increase during the high
37 productivity period, while both *N. incompta* and *G. truncatulinoides* display a higher
38 calcification during the low productivity period. The comparison of these patterns

39 with environmental parameters indicate that controls on seasonal calcification are
40 species-specific. Interannual analysis suggest that both *G. bulloides* and *N.*
41 *incompta* did not significantly reduce their calcification between 1994 and 2005,
42 while *G. truncatulinoides* exhibited a constant and pronounced increase in its
43 calcification that translated in an increase of 20% of its shell weight. The comparison
44 of these patterns with environmental data reveals that Optimum Growth Conditions
45 affect positively and negatively *G. bulloides* and *G. truncatulinoides* calcification,
46 respectively. Sea Surface Temperatures have a positive influence on *N. incompta*
47 and *G. truncatulinoides* calcification, while carbonate system parameters appear to
48 affect positively the calcification of three species in the Gulf of Lions throughout the
49 12-year time series.

50 Finally, comparison between sediment trap data and seabed sediments allowed us
51 to assess the changes of planktic foraminifera calcification during the late Holocene,
52 including the preindustrial era. Several lines of evidence indicate that selective
53 dissolution did not bias the results in any of our data sets. Our results showed a
54 weight reduction between pre-industrial and post-industrial Holocene and recent
55 data, with *G. truncatulinoides* experiencing the largest weight loss (32-40%) followed
56 by *G. bulloides* (18-24%) and *N. incompta* (9-18%). Overall, our results provide
57 evidence of a decrease in planktic foraminifera calcification in the western
58 Mediterranean, most likely associated with ongoing ocean acidification and regional
59 SST trends, a feature consistent with previous observations in other settings of the
60 world's oceans.

61

62 **Key words:** Planktic foraminifera, foraminifera calcification, biogeochemical cycles,
63 Ocean Acidification, Mediterranean Sea.

64 1. Introduction

65

66 Growing population and its linked human activity since the industrial period (defined
67 according to Sabine et al., (2004) from 1800 and therein) has caused an increase in
68 carbon dioxide, which ecological and economic consequences are considered a
69 major threat (Ipcc, 2022). Atmospheric CO₂ concentrations during the Pleistocene
70 and Holocene ranged from 200 to 280 parts per million (ppm) (Loulergue et al., 2007;
71 Lüthi et al., 2008; Parrenin et al., 2007), but these values have increased
72 dramatically since the onset of the industrial period, exceeding the threshold of 400
73 ppm in 2015 for the first time for at least the last 800.000 years (Lüthi et al., 2008).
74 This increase is significantly more important since the 1950s, when rapid
75 atmospheric changes due to human activity took place, a process referred as “Great
76 Acceleration” (Head et al., 2022a). Since then, between, 25 and 30% of

77 anthropogenic CO₂ has been absorbed by the world's ocean (Sabine et al., 2004).
78 The ocean uptake of atmospheric CO₂ causes a drop in both pH and carbonate ion
79 concentration (Barker et al., 2012), lowering seawater alkalinity; this process is
80 commonly known as Ocean Acidification (OA), and it is expected to affect all areas
81 of the ocean and to have a wide impact on marine life (Davis et al., 2017; Figuerola
82 et al., 2021; Orr et al., 2005). One of the main questions about recent environmental
83 change is how different ecosystems and regions in global ocean are going to react
84 to the ongoing increase of anthropogenic atmospheric carbon dioxide.

85 A large body of evidence indicates that ocean acidification has substantial and
86 diverse effects on the distribution and fitness of a wide range of marine organisms
87 (Kroeker et al., 2013; Meier et al., 2014; Moy et al., 2009). For example, some fleshy
88 algae and diatom species have been shown to increase their growth and
89 photosynthetic activity at enhanced CO₂ concentrations (Kroeker et al., 2013). In
90 turn, most calcifying organisms such as calcifying algae, corals, pteropods,
91 coccolithophores and foraminifera are negatively affected by this process often
92 showing a reduction in their abundance, calcification and growth rates (Kroeker et
93 al., 2013; Orr et al., 2005).

94 Planktic foraminifera are a group of marine single-celled protozoans that produce
95 calcareous shells. Their distribution across the water column is conditioned by
96 factors that include, but are not limited to, food availability, temperature, salinity and
97 sunlight (Schiebel and Hemleben, 2005). These organisms are considered to play a
98 key role in marine carbon cycle and carbonate production, accounting for between
99 32 and 80% of the deep ocean calcite fluxes (Schiebel, 2002). Depending on their
100 ecology and feeding strategies, these organisms can be algal (dinoflagellates)
101 symbiont bearing or not symbiont bearing and be spinose or non-spinose. Planktic
102 foraminifera represent a useful tool for palaeoecological and palaeoceanographic
103 studies, as the abundances of different species and their geochemical signature
104 allow reconstructing sea surface temperatures and water column physical and
105 chemical properties (Lirer et al., 2014; Margaritelli, 2020; Schiebel and Hemleben,
106 2017).

107 Previous studies suggest that planktic foraminifera are sensitive to ocean
108 acidification (OA). Laboratory experiments indicate that when carbonate ion
109 concentration decreases, shell weight and calcification decrease too in a variety of
110 species (Bijma et al., 2002; Lombard et al., 2011). Species that host symbionts have
111 been described showing a higher tolerance to dissolution due to the capacity of algal
112 symbionts to alter immediate seawater chemistry (Lombard et al., 2009). Moy et al.
113 (2009) documented a decrease of 30-35% shell weight in the planktic foraminifera
114 *G. bulloides* during the industrial era in the subantarctic Southern Ocean, most likely
115 induced by anthropogenic-driven ocean acidification. A recent study by Fox et al.

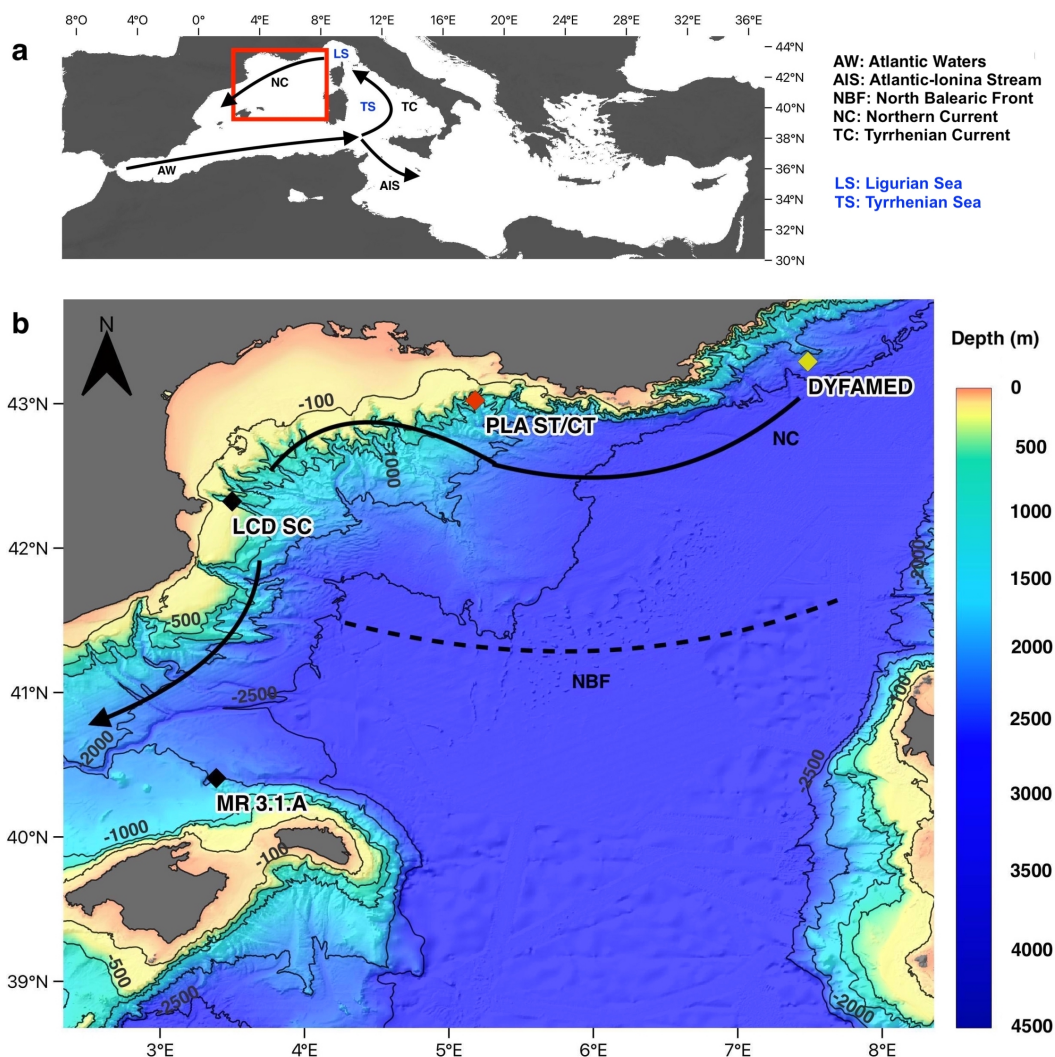
116 (2020) showed that non-spinose (*N. dutertrei*) foraminifera species exhibit a more
117 pronounced calcification reduction than the spinose (*G. ruber*) species in response
118 to increasing CO₂. The main difficulty for studying the impact of OA on foraminifera
119 (and any calcifying organisms) resides in finding long-term continuous records in
120 order to be able to evaluate possible changes in shell calcification (Fox et al., 2020).
121 In order to assess the impact of recent environmental change on planktic
122 foraminifera, in this work we present data from Planier sediment trap (data from 1993
123 to 2006) (Rigual-Hernández et al., 2012) and from seabed sediments from three
124 different sites located in both the Gulf of Lions and the promontory of Menorca. The
125 Mediterranean Sea is a semi-enclosed sea with a high saturation state for calcite
126 (Álvarez et al., 2014). It is often considered as a “miniature ocean” and a “laboratory
127 basin” (Bergamasco and Malanotte-Rizzoli, 2010) which makes it a valuable zone to
128 study the response of marine calcifying organisms to environmental change.
129 The advantage of sediment traps is that they can provide data coming from annual
130 fluxes, avoiding the effects of seasonal abundance and ontogeny and making
131 interannual comparisons more reliable (Jonkers et al., 2019). Three different planktic
132 foraminifera species, each of which characterized by contrastingly different depth
133 habitats and ecologies, were selected for our analysis: *G. bulloides*, a spinose
134 opportunist surface dweller that lies above the thermocline (Schiebel and Hemleben,
135 2014); *N. incompta*, a non-spinose temperate surface dweller; and *G.*
136 *truncatulinooides*, a non-spinose deep dwelling species which migrates through the
137 water column with a complex life cycle. Our aims for this study are: (i) to compare
138 two widely used foraminifera weighing and size-normalization techniques and
139 provide a baseline of modern foraminifera weight data and calcification in the
140 Western Mediterranean against which future changes in foraminifera calcification
141 can be assessed (ii) document seasonal and interannual trends in the planktic
142 foraminifera calcification of the three planktic foraminifera species, and (iii) evaluate
143 possible changes in shell calcification through the Holocene to the present day by
144 comparing shell weights of the foraminifera collected by the traps with those of the
145 seafloor sediments.

146 2. Study area

147

148 The Mediterranean is a semi-enclosed sea and is considered a concentration basin
149 (Bethoux et al., 1999) with a negative hydrological budget: fresh water inputs do not
150 compensate the overall basin evaporation. The surface oceanic waters that enter
151 the Mediterranean through the Strait of Gibraltar and spread towards the eastern
152 basin compensate this negative balance. The waters of Atlantic origin (AW) circulate
153 according to a cyclonic circuit (counterclockwise) along the Mediterranean rim (Fig.

154 1a). In the northwestern basin, this along-slope current, called the northern current
 155 (NC), is formed by the convergence at the level of the Ligurian Sea (LS) of the waters
 156 flowing on both sides of Corsica. The general circulation in this sub-basin forms a
 157 cyclonic pattern, flowing westward along the Gulf of Lions, bypassing the Balearic
 158 Sea and finally closing its circuit eastward along the North Balearic Front (NBF) (Fig.
 159 1b).



160

161 **Figure 1. a.** Study area location in the Mediterranean Sea and general
 162 surface circulation **b.** geographic setting of the Gulf of Lions and location of
 163 studied sites. Red diamond shows the position of the Planier site sediment
 164 trap and core-top (PLA ST/CT). Black diamonds represent the location of the
 165 seabed sediments samples analyzed from Lacaze Duthiers canyon (LCD SC)
 166 and Menorca promontory (MR 3.1A). Yellow diamond represents the location
 167 of the Dynamics of Atmospheric Fluxes in the MEDiterranean Sea
 168 (DYFAMED) site, located 200 km upstream Planier station position. Arrows

169 represent the surface circulation (Millot, 1999). The topographic model was
170 downloaded from the GEBCO database.

171 Moreover, the Mediterranean is recognized as a sensitive region to increasing
172 atmospheric CO₂ due to the fast turnover time of its waters (Béthoux et al., 2005)
173 and the fast penetration of anthropogenic CO₂ (Schneider et al., 2007). Sea surface
174 temperatures are predicted to increase by 1.5-2°C by the end of the century, a faster
175 rate than the global average (Lazzari et al., 2014). pH is expected to decrease
176 according to the global average (0.3-0.4 units by 2100) or even exceed the global
177 trend (Hassoun et al., 2015). The Mediterranean Sea is also affected by other
178 stressors, which impact marine organisms in many ways (Lejeune et al., 2009).
179 Finally, it is also a region shaped by human development and its associated activities
180 interact with environmental changes (Mediterranean Experts on Climate Change,
181 MedECC, 2019).

182 The Gulf of Lions is located in the northwestern part of the Mediterranean Sea, and
183 its morphology presents a continental slope with an array of complex submarine
184 canyons (Rigual-Hernández et al., 2012) (Fig. 1b). Vertical mixing, generated by
185 intense surface cooling and evaporation, occurs in winter in the Gulf of Lions driven
186 by cold, dry northern winds, resulting in dense water on the shelf and offshore
187 (Durrieu de Madron et al., 2005; Houpert et al., 2016; Millot, 1990). This winter mixing
188 recharges surface waters with nutrients. This enrichment with increased solar
189 radiation stimulates primary production in spring. Increasing heat fluxes during
190 spring and summer cause water mass stratification and nutrient depletion, which
191 lasts until late summer, until fall cooling breaks the stratification of the water column
192 and causes a fall bloom (Heussner et al., 2006; Monaco et al., 1999; Rigual-
193 Hernández et al., 2012). River inputs are the main source of suspended particles in
194 the Gulf of Lions, and the Rhone river represents the most important river in the
195 northwestern Mediterranean; however, other sources include Saharan dust deposits
196 and biological production (Heussner et al., 2006; Monaco et al., 1999). Overall, the
197 oceanographic setting of the Gulf of Lions is an exception to the general oligotrophy
198 of the Mediterranean Sea.

199 3. Material and methods

200

201 3.1. Sediment traps, core-tops and sediment cores.

202 A series of deployments of sediment traps mooring lines in the Gulf of Lions
203 continental margin was initiated in 1993 within the framework of several French and
204 European projects (PNEC, Euromarge-NB, MTP II-MATER, EUROSTRATAFORM)
205 and the monitoring of two sites, Planier and Lacaze-Duthiers stations (Fig. 1),
206 continues as a component of the MOOSE program (Mediterranean Ocean

207 Observing System for the Environment) (Coppola et al., 2019). Planier station
 208 (43°02'N, 5°18'E) is located at the northeastern end of the Gulf of Lions, in the axis
 209 of the Planier Canyon. The sediment trap used for this work was located at around
 210 530 m water depth in a water column of ~1000m. Further details of the mooring
 211 design can be found in Heussner et al., (2006). Planktic foraminifera fluxes for the
 212 1993 to 2006 period were documented by Rigual-Hernández et al., (2012). Here, we
 213 used the samples from the latter study for our weight and calcification analysis. This
 214 sediment trap is used here as a baseline of the planktic foraminifera dwelling in the
 215 modern Mediterranean Sea. Moreover, we analyzed a set of core top and sediment
 216 cores collected from several locations of the Northwestern Mediterranean that are
 217 considered to represent foraminifera assemblages sedimented during the Holocene
 218 era (Table 1).

219 **Table 1.** Description of the core tops used in this study. Data for Planier core-
 220 top (PLA CT) and Lacaze-Duthiers sediment core (LCD SC) are available in
 221 Heussner et al., (2006), and data concerning Menorca sediment core (MR
 222 3.1.A) can be found in Cisneros et al., (2016). Conventional ¹⁴C ages, 1-sigma
 223 uncertainties, local reservoir and the calibrated age have been rounded
 224 according to convention. See section 3.7 for details concerning “Bomb ¹⁴C”.

Site	Location	Water depth (m)	Sediment Samples	Samples Depth (cm)	Sample dated	Species dated	Radiocarbon age (¹⁴ C years BP)	1-sigma error (¹⁴ C years)	Local reservoir (¹⁴ C years BP)	Calibrated age (cal. years BP)
PLA CT	42.989° N 5.121° E	1095	2	0-1	0.5-1 cm	<i>G. bulloides</i>	490	60	165 ± 95	Bomb ¹⁴ C
LCD SC	42.265°N 3.54°E	990	7	0-5	0.5-1 cm	<i>G. bulloides</i>	460	60	165 ± 95	Bomb ¹⁴ C
MR 3.1.A	40.29°N 3.37° E	2117	40	0-27	14-14.5 cm	<i>G. bulloides</i>	1980	65	165 ± 95	1560

225

226 3.2. Sediment core samples processing

227 A total of 2 sediment samples from Planier core top, 7 from Lacaze-Duthiers
 228 sediment core and 40 from Minorca sediment core were weighed (Table 1). Dry bulk
 229 sediment samples from all sites was weighed using a Sartorius CP124S balance
 230 (precision= 0.1mg).

231 The samples were then wet-sieved in order to separate the <63 μm fraction and dry
 232 sieved to separate the bigger fractions (>150 μm and >300 μm). The sediment
 233 washing was carried out with potassium phosphate-buffered solution (pH= 7.5) in
 234 order to optimize foraminifera preservation. Each fraction was oven dried at a
 235 constant temperature (50°C) and then weighed. The >150 μm fraction was used for
 236 identification, counting and shell morphometric and weight analyses.

237

238 **3.3. Ecology and life cycle of *Globigerina bulloides*, *Neogloboquadrina***
239 ***incompta* and *Globorotalia truncatulinoides***

240 *G. bulloides* is a spinose surface to sub-surface dweller (Schiebel and Hemleben,
241 2017a), found in the upper 60 m of the water column. This species has affinity for
242 temperate to sub-polar waters and upwelling systems in lower to mid latitudes
243 (Azibeiro et al., 2023; Bé et al., 1977). In terms of its seasonal distribution, it has
244 been documented to be associated to enhanced productivity periods in mid to high
245 latitudes (Chapman, 2010; Schiebel and Hemleben, 2005). No symbiont algae are
246 hosted by this species and, contrary to most spinose species, its diet is mainly algae
247 based (Schiebel et al., 2001). *G. bulloides* shows an opportunistic feeding and
248 strategy, leading to a high abundance in the foraminifera assemblages preserved in
249 the sedimentary record. This is despite having a tests that has been documented to
250 be more susceptible to dissolution than the average of the planktic foraminifera
251 species (Dittert et al., 1999).

252 *N. incompta* is a surface dweller abundant in subpolar to temperate water masses
253 across all the ocean basins (Kuroyanagi and Kawahata, 2004). It is a non-spinose
254 species and does not carry symbiont algae. In North-Atlantic waters, *N. incompta* is
255 a major component of foraminifera assemblages from late spring to late fall, and
256 generally, is the dominant foraminifera species during late summer when maximum
257 shoaling of mixed layer depths occur (Schiebel and Hemleben, 2000). It shows a
258 minor presence in low latitudes and during periods of enhanced nutrient supply, *N.*
259 *incompta* is outnumbered by other more opportunistic species (Schiebel et al., 2002).

260 *G. truncatulinoides* is considered the deepest dweller among the extant planktic
261 foraminifera, with living specimens documented below 2000 m (Schiebel and
262 Hemleben, 2005). Considered a widespread species, it can be found from subpolar
263 to subtropical water masses (Schiebel and Hemleben, 2017). It is a non-spinose
264 species (Margaritelli, 2020), and it does not carry any symbiont algae (Takagi et al.,
265 2019). An important aspect to highlight about this species is its complex life cycle
266 (Margaritelli et al., 2022). It reproduces once a year in the upper water column during
267 late winter, when mixing of the water column allowed the migration of juveniles to
268 the surface waters (Lohmann and Schweitzer, 1990; Schiebel et al., 2002). The
269 former authors speculated that nutrient availability and the avoidance strategies to
270 predation could explain this its life cycle. Then, the adult migrate downward the water
271 column (Rebotim et al., 2017) and spend the rest of their life cycle developing an
272 additional calcite layer in cooler waters below the thermocline (Lohmann and
273 Schweitzer, 1990; Wilke et al., 2009). Around 70% of *G. truncatulinoides* calcification
274 has been estimated to take place around the thermocline, while the remaining 30%
275 take place in surface waters (LeGrande et al., 2004).

276 The abundance of these three species has been previously studied in the Gulf of
277 Lions by Rigual-Hernández et al., (2012). The latter study showed that both *G.*
278 *bulloides* and *N. incompta* displayed their maximum abundances during the spring
279 bloom, while *G. truncatulinoides* abundance was maximum during early winter. On
280 the other hand, minimum abundances were reached during late spring and summer
281 for *G. bulloides* and *N. incompta* respectively, and *G. truncatulinoides* displayed a
282 minimum abundance during fall.

283

284 **3.4. Foraminifera picking and mass and size estimations**

285 Different sizes were selected depending on the maximum availability of each
286 species: 250-300, 200-250 and 400-500 μm for *G. bulloides*, *N. incompta* and *G.*
287 *truncatulinoides*, respectively. For the latter species, both coiling morphotypes were
288 selected although the right coiling was substantially less abundant representing less
289 than 3% in our counts, a feature consistent with the literature that indicates a low
290 presence of right coiled specimens (Margaritelli et al., 2020; 2022).

291 A total of 273 foraminifera samples were picked for this study, 126 coming from the
292 sediment trap and 147 from the three sediment cores and core tops (Table 2).
293 However, these numbers represent the total of samples analyzed but unique
294 samples number is lower, as not all the sediment trap samples presented the three
295 species in high enough numbers to perform the picking. The species were analyzed
296 in size fractions in order to estimate the efficiency of sieve fractions and the impact
297 of size and morphometric parameters on the foraminifera weight and calcification.
298 The mean weight of each available sediment trap sample was obtained by weighting
299 between 15 to 45 specimens of *G. bulloides* (mean N= 27), 5 to 25 *N. incompta*
300 (mean N= 15) and 5 to 25 *G. truncatulinoides* (mean N= 13). Concerning the
301 analyses of the core top and sediment core samples, between 15 and 25 *G. bulloides*
302 and *N. incompta* (mean N= 20 for both) and between 9 and 25 *G. truncatulinoides*
303 (mean N= 18) were picked.

304 Each foraminifera sample was then exposed to gentle ultrasonication (50 Hz) for 5
305 to 75 seconds (depending on the species and the degree of visual uncleanliness) in
306 methanol in order to clean the shells. The samples were then left to dry in a
307 temperature-controlled oven at 50°C. One out of three analyzed samples were
308 weighted before and after cleaning in order to assess potential shell mass losses
309 and shell preservation due to ultrasonication. Our results indicate that this method
310 has little impact on shell preservation with around 95% of the total foraminifera
311 conserved in good conditions. Weight loss between non-cleaned samples and
312 cleaned samples is a mean 0.5 to 3 μg (between 6 and 32% of the sample total
313 measured weight) depending on the species, mainly due to the presence of clay and

314 non-calcite material in the shells, which justifies this cleaning process (see
315 Supplementary fig. 6).

316 The weightings were carried in the micropaleontology laboratory of the Geology
317 Department at University of Salamanca using a Sartorius ME5 balance (precision=
318 0.001 mg). This method allowed us to obtain foraminifera Sieve Based Weight
319 (SBW) by dividing the average shell weight per sample (5-45 tests) by the total
320 number of foraminifera within each sample. The lowest number of individuals
321 selected per sample was five in order to maximize the number of samples available
322 for our study. According to Beer et al., (2010), the higher the number of individuals,
323 the more reliable SBWs are. Here we aim to compare SBW results with a measured
324 weight technique. Measured techniques are acknowledged to be reliable with a lower
325 number of individuals, therefore a minimum of five individuals were selected in order
326 to compare the two techniques.

327 However, it has been described that traditionally used sieve fractions method is
328 considered unreliable because of the effect of morphometric parameters on the
329 foraminifera weight (Beer et al., 2010). In order to remove the size effect on the
330 weight, the mean SBW was normalized to the mean diameter and area of the
331 planktic foraminifera to obtain Measurement Based Weights (MBW). Morphometric
332 parameters were measured using a Nikon SMZ18 stereomicroscope equipped with
333 a Nikon DS-Fi3 camera and NISElements software. These measurements were
334 carried out on the same shells that were weighted. Foraminifera shells were
335 positioned in order to obtain the maximum area of each individual, in this case, the
336 umbilical side (aperture facing upwards) was measured for the three species.

337 MBW_{area} and $MBW_{diameter}$ were calculated according to the following formula
338 (Aldridge et al., 2012; Beer et al., 2010), where “parameter” accounts for “area” or
339 “diameter”:

340

$$341 \quad MBW_{sample} = \frac{mean\ SBW_{sample} \times mean\ parameter_{size\ fraction}}{mean\ parameter_{sample}}$$

342

343 “Size fraction” accounts for the mean of the parameter (area or diameter) measured
344 in all the sites studied, while “sample” accounts for the mean of the parameter in the
345 particular sample being measured. The advantage of these measurements is that
346 the resulting MBW is being given with a weight unity (μg), thereby allowing direct
347 comparison with other studies (Beer et al., 2010) and useful for estimating their
348 contributions to marine biogeochemical cycles.

349 Correlations between SBW and MBW_{area} against area are displayed in Fig. 2. The
350 reason for this comparison is to show the relation between size and weight and to

351 avoid the effect of having the bigger specimens displaying the heaviest weight and
352 impacting the mean weight (therefore calcification indicator) of the sample.
353 Finally, in order to compare weights patterns from the sediment trap with weights
354 from core tops and sediment cores and overcome the seasonality effect, MBWs were
355 flux-weighted. Mean monthly MBWs values from each species were multiplied by
356 the corresponding mean monthly flux and then divided by the total annual flux of the
357 corresponding species. For these calculations, the flux data from each species
358 estimated for the >150 μm fraction from Rigual-Hernández et al., (2012) was
359 employed.

360

361 **3.5. Environmental data**

362 Foraminifera fluxes and abundances together with chlorophyll-a were taken from
363 Rigual-Hernández et al., (2012) for the entire time span of the analyzed samples.
364 Both fluxes and abundance come from direct sediment observation from the Planier
365 site, while chlorophyll-a data was obtained from SeaWiFS monthly measurements
366 through NASA's Giovanni program on a $0.2 \times 0.2^\circ$ area around the mooring location.
367 SeaWiFS measurements started in 1997 and were used due to the lack of direct
368 chlorophyll measurements in our samples. Sea Surface Temperature (SST) was
369 recovered from the NOAA database with the same gridding as the data from the
370 NASA's Giovanni program.

371 Salinity, nutrient concentrations (nitrates and phosphates) and carbonate system
372 parameters data were collected from the DYFAMED database ([http://www.obs-
374 vlfr.fr/dyfBase/index.php](http://www.obs-
373 vlfr.fr/dyfBase/index.php)) (Coppola et al., 2008; 2021). DYFAMED site is located
375 around 200-220 km (Fig. 1b) east of the sediment trap location ($43^\circ 25' \text{N}$, $7^\circ 52' \text{E}$), in
376 the Ligurian Sea. From an oceanographic view, its situation is upstream of the NC
377 circulation and can be considered representative of seasonal and interannual
378 variability of biological and water column properties of the open-ocean waters in the
379 northwestern Mediterranean (Heussner et al., 2006; Meier et al., 2014). Alkalinity
380 and total carbon measurements were available for years 1998 to 2000 and mid 2003
381 to 2005. Missing values comprised in these years were replaced with values
382 obtained from linear regression of the measurements from above and below. The
383 CO2SYS macro has been used to reconstruct the $[\text{CO}_2]$, $[\text{CO}_3^{2-}]$, $[\text{HCO}_3^-]$ and pH
384 values from the measured total alkalinity and dissolved inorganic carbon. The
385 constants used were the CO_2 dissociation constant by Mehrbach et al., (1973) refit
386 by Dickson and Millero, (1987); the KHSO_4 by Dickson, (1990); and the seawater
387 scale for pH.

388

388 **3.6. Statistical analysis**

389 In order to have uninterrupted monthly environmental values from the DYFAMED
390 site during available measurements, a resampling every 10 days has been carried
391 out with the QAnalySeries program.

392 Independence and correlation between the area the different species SBWs and
393 MBW_{area} was tested using a Pearson linear correlation test with an R script (see
394 Supplementary material).

395 Seasonal correlation analyses were carried out with the Statistica program. A $p < 0.05$
396 was used in order to consider a correlation as significant. The number (N) of
397 correlations depended on data availability and was 10 for *G. bulloides*, 9 for *N.*
398 *incompta* and 12 for *G. truncatulinoides*.

399 It should be noted that the analysis of interannual trends was hindered by gaps in
400 the sediment trap record and by the low number of specimens during some sampling
401 intervals. Therefore, interannual trends in planktonic foraminifera calcification should
402 be interpreted with caution.

403 The influence of environmental variables upon MBW_{area} was assessed using
404 General Additive Models (GAM) (fitted using the *gam* function from the *mgcv* R
405 package). Due to data limitation, the GAMs could not be fitted to multiple
406 independent variables, so potential effects of interacting environmental variables
407 were could not be assessed. Each model tested the dependence of the different
408 MBW upon a single independent variable: month or year, to evaluate seasonal and
409 interannual trends; the flux of each species, to test effects of ecological variability;
410 and a suite of environmental variables to determine impacts of various aspects of
411 ocean chemistry on the calcification. Smooth functions of these measured quantities
412 were used as the single independent variable within the GAMs, which were fitted
413 using the default settings of the *gam* function: a Gaussian family and identity link
414 function; and the GCV.cp smoothing method. GAM results quantified the
415 significance of the effect of each independent variable upon MBW.

416 In order to investigate the difference between the MBW data from the sediment trap
417 and the core-top /sediment cores, a non-parametric two-way Mann-Whitney test has
418 been performed. This test determines if there are significant differences in the
419 medians of data sets without making assumptions about the data distributions. A p -
420 value < 0.05 has been used to consider the median of two datasets different.

421

422 **3.7. Radiocarbon dating**

423 Between 50-100 individuals of well-preserved *G. bulloides* shells ($> 150 \mu\text{m}$) were
424 picked for radiocarbon analyses. Radiocarbon ($^{14}\text{C}/^{12}\text{C}$) was measured as CO_2 with
425 a gas ion source in a Mini Carbon Dating System (MICADAS) at the Laboratory of
426 Ion Beam Physics from ETH Zürich. The employed automated method consists of
427 initial leaching of the outer shell to remove surface material with $100 \mu\text{l}$ of ultrapure

428 HCl (0.02M) and the subsequent acid digestion of the remaining carbonates with
429 100 µl of ultrapure H₃PO₄ (85%) (Wacker et al., 2013). Therefore, no cleaning was
430 applied after the picking contrary to the samples used for mass and size
431 measurements. Marble (IAEA-C1) was used for blank correction and results were
432 corrected for isotopic fractionation via ¹³C/¹²C isotopic ratios.

433 Conventional radiocarbon age for sample 14-14.5cm from MR 3.1.A site was
434 calibrated with the on-line calibration program CALIB (Stuiver and Reimer, 1993)
435 using the Marine20 curve, which applied a marine reservoir correction of 550 ¹⁴C
436 years (Heaton et al., 2020) to the corresponding ¹⁴C age and error. Additionally, a
437 local reservoir effect (Stuiver and Braziunas, 1993) of -165 ± 95 ¹⁴C years was
438 considered. This local reservoir was calculated as the average of the 8 nearest
439 points to the sample location from the Marine Reservoir Correction database
440 (Reimer and Reimer, 2001), whose values have already been corrected for the
441 Marine20 curve. ¹⁴C ages from samples 0.5-1cm from both PLA CT and LCD SC
442 lied out of the range for calendar calibration, implying these samples contain some
443 bomb ¹⁴C and cannot be considered pre-industrial (Table 1, see “bomb ¹⁴C”). In order
444 to have an estimation of the time span that could be covered by these dates, the
445 same marine and local reservoir corrections were applied to the most recent ¹⁴C date
446 that could be corrected (i.e. 603 ¹⁴C years BP). As the F¹⁴C for this sample was <1
447 (see Supplementary table 1), this means that the ¹⁴C found in these samples is not
448 dominated by the bomb carbon. Here we propose a 110-50 cal. years BP age for
449 these samples. Then, these samples could be considered post-industrial. The
450 detailed results of the calibration and the ¹⁴C dating can be found in the
451 Supplementary figs. 1 and 2.

452 Finally, it is important to consider that these ¹⁴C ages represent mean average
453 values. Therefore, time integration within each sample and the effects of bioturbation
454 could cause a variation on the foraminifera real ages (Dolman et al., 2021).

455 Both the samples and dates obtained are detailed in Table 1. Planktic foraminifera
456 present in the dated samples that were not selected for radiocarbon dating were also
457 analyzed following the methodology described previously.

458 4. Results

459

460 4.1. Shell morphometric parameters and shell-weight normalization

461 **Table 2.** Minimum, mean, maximum and standard deviation values of shell
462 area, diameter and SBW for *G. bulloides*, *N. incompta* and *G. truncatulinoides*
463 at all studied sites. The last 3 columns show the number of samples, the mean
464 number (N) of individuals analyzed per sample and the total number of
465 individuals measured for each site.

PLA Sediment Trap	Area (μm^2)				Diameter (μm)				Sieve Based Weight (SBW, μg)				Total	N per	total
	Min	Mean	Max	Std.Dev	Min	Mean	Max	Std.Dev	Min	Mean	Max	Std.Dev	samples	sample	N
<i>G. bulloides</i>	16978	57353	168492	17261	147.0	267.5	463.2	38.6	3.21	4.43	5.60	0.66	35	27.2	893
<i>N. incompta</i>	26234	42821	135422	8934	182.8	232.4	415.2	22.6	3.17	4.45	5.40	0.59	32	15.0	455
<i>G. truncatulinoides</i>	70712	178952	527622	63572	291.9	468.5	819.6	81.9	10.67	23.11	39.57	7.79	59	13.0	729
PLA Core-Top															
<i>G. bulloides</i>	37163	55395	87894	12302	217.5	264.0	334.5	28.8	5.00	5.22	5.43	0.30	2	17.3	39
<i>N. incompta</i>	27635	36927	49619	5447	187.6	216.3	251.4	15.9	4.46	4.46	4.46	0.00	2	19.7	41
<i>G. truncatulinoides</i>	89778	174748	233229	44313	338.1	467.7	544.9	61.9	34.80	35.40	35.90	0.70	2	14.7	34
MIN Sediment core															
<i>G. bulloides</i>	20895	52132	138424	8722	163.1	256.8	419.8	20.5	4.00	5.07	6.57	0.46	40	19.6	761
<i>N. incompta</i>	24003	35098	57264	4658	174.8	211.0	270.0	13.7	3.45	4.11	5.00	0.34	40	20.3	791
<i>G. truncatulinoides</i>	116686	166318	365851	23262	385.4	459.1	682.5	30.8	28.33	34.99	42.60	3.25	40	14.4	576
LCD Sediment core															
<i>G. bulloides</i>	27624	52472	116605	8793	187.5	257.7	385.3	20.4	4.35	4.73	5.19	0.31	7	20.1	136
<i>N. incompta</i>	28089	37789	51284	4972	189.1	218.9	255.5	14.4	3.68	4.12	4.50	0.26	7	19.8	134
<i>G. truncatulinoides</i>	82534	143138	393754	41620	324.2	423.3	708.1	55.9	25.27	26.68	30.66	1.94	7	15.3	105

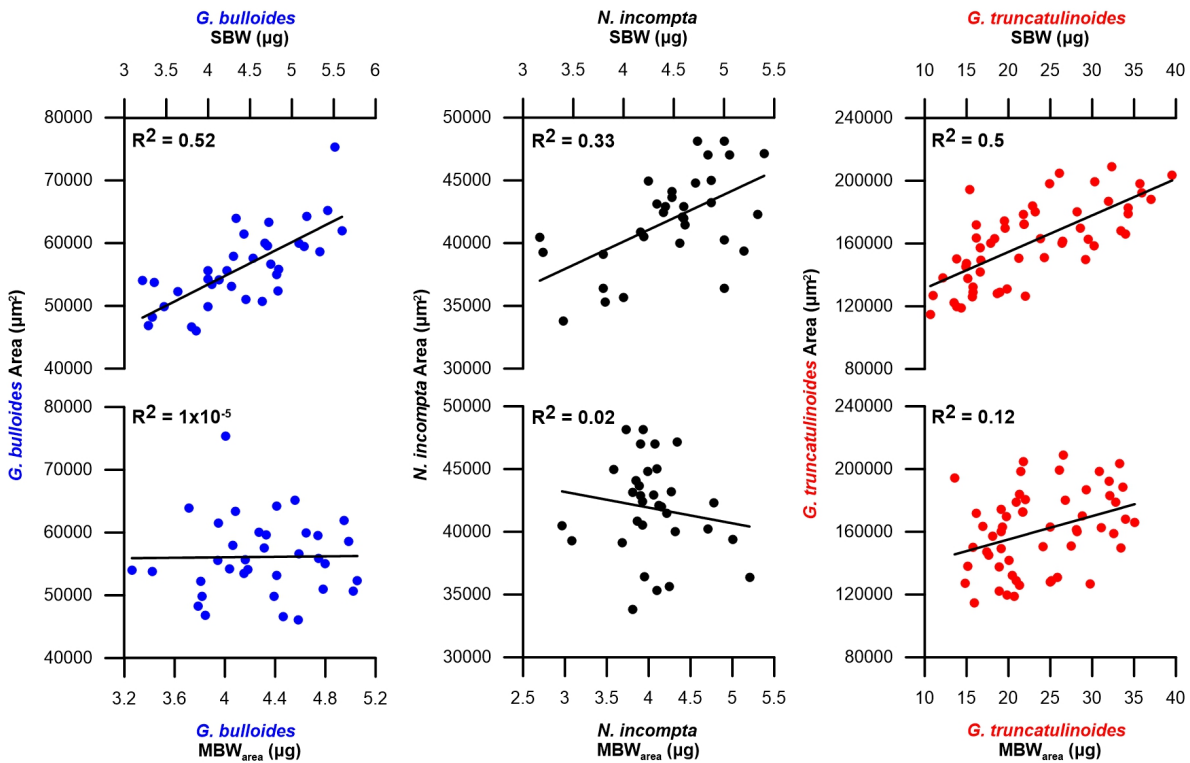
466

467 Overall, the mean values for both diameter and area correspond to the mean
468 narrowed size fraction used during the picking, but morphometric parameters show
469 some variability between the studied sites. Standard deviation of both area and
470 diameter values for the three species are higher in the sediment trap record than in
471 seafloor sediments, with mean values (of all three species) of 82% higher for area
472 and 69% higher for diameter. SBW exhibits the same pattern as both area and
473 diameter standard deviation is a mean 130% higher in the Planier sediment trap.
474 Regarding the variability across the seafloor samples, Planier core-top exhibits a
475 greater area and diameter values (about 40 to 50% increase for the three species)
476 compared to those of the other two sediment cores, probably due to the fewer
477 samples analyzed (Table 2).

478 The Planier sediment trap results (Table 2) show a higher standard deviation for both
479 area and diameter for the three species, i.e. 76 % and 68% higher for *G. bulloides*
480 compared to the data from core tops, 78% and 54% for *N. incompta* and 81% and
481 73% for *G. truncatulinoides*.

482 Because of the lack of precision of the initial individuals picking, carried out with a
483 micrometer installed in the microscope, the selection is not totally accurate. Due to
484 this issue, one third of the of the total measured foraminifera (i.e. 1645 of 4694) were
485 out of the desired size fraction, of which 12% were bigger (580/4694) and 23% were
486 smaller (1065/4694). Nonetheless, only 0.02% were more than 20% out of the
487 selected size range (64/4694 more than 20% bigger and 29/4694 more than 20%
488 smaller). Mean size difference for the foraminifera out of the size fraction is around
489 7%. Results vary according to the site and the species. 50% of the individuals from

490 the Planier sediment trap (1046/2077) and 26% of the individuals coming from the
 491 core tops (692/2617) were out of range. *G. bulloides* showed a 45.5% (53.2% in the
 492 sediment trap and 39.3% in the core-tops samples) of individuals out of selected size
 493 fraction, while this value was 21.5% (22.2% in sediment trap, 21.1% in sediment
 494 cores) for *N. incompta* and 35% for *G. truncatulinoides* (53.4% in sediment trap,
 495 16.7% in sediment cores).
 496 Even though a narrow size class was selected for each species (see section 3.4), a
 497 clear influence of the area on the SBW was found in our data set (Fig. 2).
 498



499

500 **Figure 2.** SBW in μg and MBW_{area} in μg against the mean test area in μm^2 for
 501 foraminifera samples in the Planier sediment trap. Dark blue dots correspond
 502 to *G. bulloides*, black dots to *N. incompta* and red dots to *G. truncatulinoides*.

503 In particular, SBW shows a positive correlation with area: $0.33 < r^2 < 0.53$ (Fig. 2). This
 504 indicates that the SBW is dependent on the size of the specimens within the selected
 505 size range. Thus, to isolate the component of variation in foraminifera shell thickness
 506 that represents a change in calcification and does not occur as a direct result of
 507 changes in shell size, normalization of the shell weight was performed following the
 508 formula detailed in section 3.3. (Beer et al., 2010). After normalization MBW_{area}
 509 shows no correlations with area: $1 \times 10^{-5} < r^2 < 0.12$ (Fig. 2). Note that the weight
 510 variations in our dataset are quite considerable, especially for *G. truncatulinoides*,
 511 probably due to the wider size fraction. Diameter does show correlation with SBW:

512 0.33<r²<0.5; and shows a non-negligible correlation with MBW_{diam}: 0.2<r²<0.33. Our
 513 data demonstrates that SBW correlates more strongly with MBW_{diam} than with
 514 MBW_{area} for the 3 species: 0.9>0.48 for *G. bulloides*, 0.89>0.52 for *N. incompta* and
 515 0.97>0.81 for *G. truncatulinoides*. These values are consistent with previous studies
 516 (Beer et al., 2010).

517 **Table 3.** Pearson correlation test results for the three species correlation
 518 between area (μm²) and both SBW (μg) and MBW_{area} (μg). Here c.i. stands
 519 for “confidence interval”. Significant r values (0<c.i.<1) are set in bold.

	Area (μm ²)					
	<i>G. bulloides</i>		<i>N. incompta</i>		<i>G. truncatulinoides</i>	
	r	c.i.	r	c.i.	r	c.i.
SBW (μg)	0.72	0.52, 0.85	0.57	0.28, 0.77	0.62	0.41, 0.76
MBW_{area} (μg)	0.014	-0.32, 0.35	-0.15	-0.47, 0.21	0.21	-0.09, 0.44

520
 521 Furthermore, a Pearson correlation test (see section 3.6) has been carried out in
 522 order to assess the influence of area on SBW and MBW_{area} (Table 3). Results
 523 showed that the SBWs from the three species correlated positively and significantly
 524 (0<c.i.<1). With their corresponding areas (0.57<r<0.72). Concerning the MBWs,
 525 no significant (0>c.i.>1) correlations with the area are observed (-0.15<r<0.2).
 526 Therefore, these correlations further highlight the fact that SBW values are
 527 significantly influenced by shell area, while MBW_{area} values appeared to be
 528 independent of the area.

529 Differences between SBW and both MBW_{area} vary depending on the species: SBW
 530 is slightly heavier for *G. bulloides*, heavier for *N. incompta* and lighter for *G.*
 531 *truncatulinoides*. The mean standard deviation for all 3 species is around 8%: 7.8%
 532 for *G. bulloides*, 6.4% for *N. incompta* and 13% for *G. truncatulinoides*. We take
 533 these values as the error adjustment for SBW in the different size fractions (250-300
 534 μm, 200-250 μm and 400-500 μm respectively). It is difficult to compare these results
 535 with other studies as size fractions and species are often different, but this error
 536 estimates are in the same order of magnitude as some other MBW published in core-
 537 tops records and sediment traps (de Moel et al., 2009; Moy et al., 2009).

538 These findings highlight the fact that the use of sieve fractions does not provide
 539 enough control on the influence of morphometric parameters in test weight.
 540 Morphometric variations described in Table 1 indicate that the typically used sieve
 541 fractions may be unreliable due to the number of individuals out of the desired
 542 fractions and the variability within the size range. The correlations between SBW
 543 and shell area are consistent with previous studies (Aldridge et al., 2012; Beer et al.,
 544 2010) and underscore the importance of isolating the component of variation in

545 foraminifera shell thickness that represents a change in calcification and does not
546 occur as a direct result of change in shell size. Thus, the shell weight was size-
547 normalized after Beer et al., (2010) by isolating the influence of isometric scaling on
548 wall thickness and calcification density.

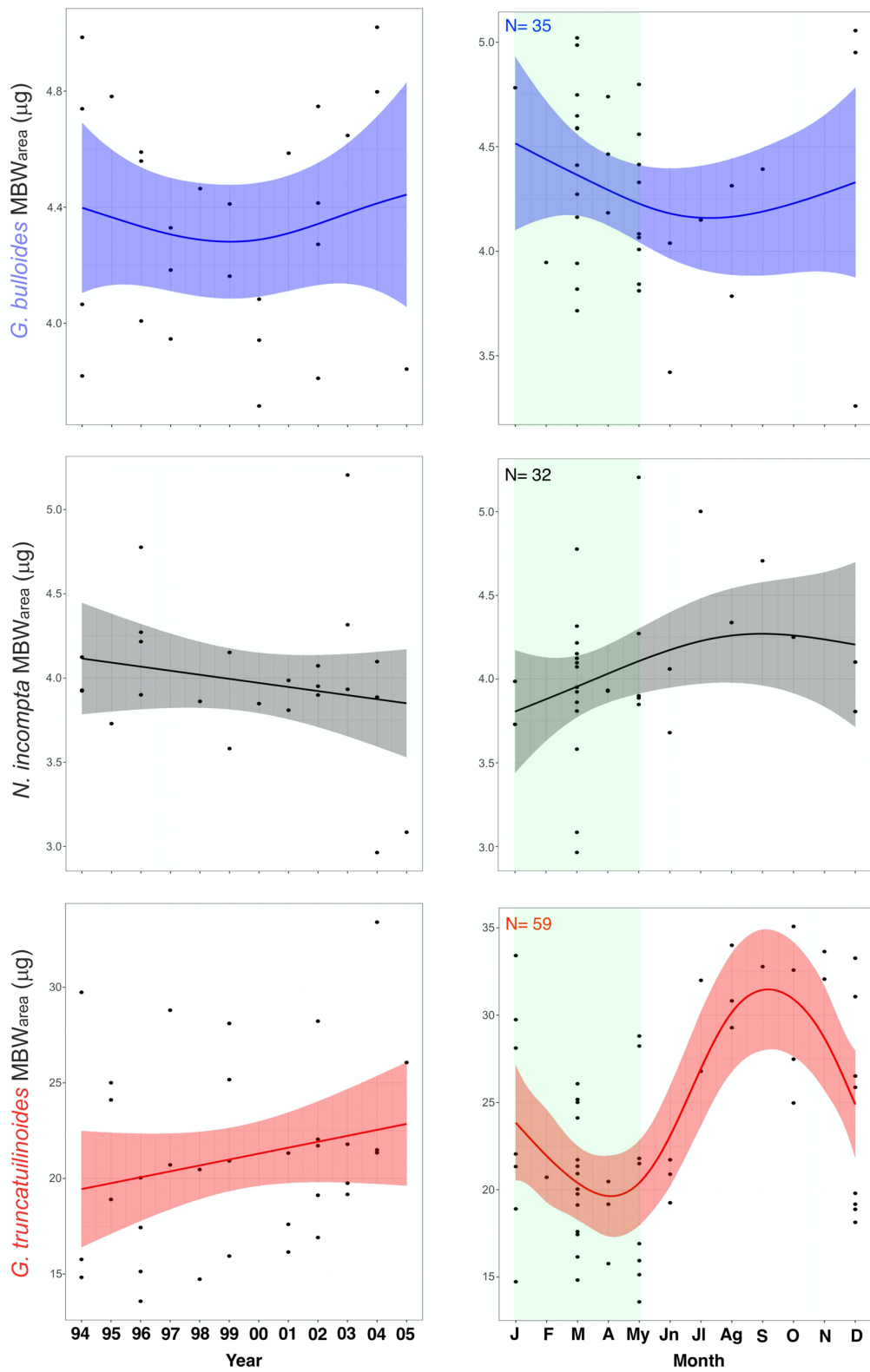
549 Moreover, both MBW_{area} (Fig. 2) and MBW_{diam} , in either the sediment trap data and
550 core-top data, do not correlate with area and diameter ($1 \times 10^{-5} < r^2 < 0.33$ and 0.001
551 $< r^2 < 0.2$ respectively) indicating that size does not have an influence on these
552 values. This suggests that our size-normalization procedure adequately removes the
553 size influence (Fig. 2) and therefore, our MBW data represents a robust parameter
554 reflecting test wall thickness and calcification intensity not influenced by test size
555 (Table 3). Therefore, MBWs can be considered as a reliable calcification intensity
556 proxy.

557 Based on all the above, from this point we'll focus our discussion on the MBW_{area} to
558 discuss the foraminifera shell weight variability on seasonal, interannual and pre to
559 post-industrial Holocene time scales.

560

561 **4.2. Seasonal variations of foraminifera calcification in the NW Mediterranean**

562 MBW_{area} values were calculated for the three species to illustrate the seasonal
563 variability of these parameters (Figs. 3 and 4). Samples have been assigned to their
564 corresponding month according to the mean cup sampling date.



565

566

567

Figure 3. Mean MBW_{area} (µg) values across the years and for a composite year for *G. bulloides*, *N. incompta* and *G. truncatulinoides* in the Planier

568 sediment trap. Light-green shaded area represents the high productivity
569 period in the study zone (Rigual-Hernández et al., 2012).

570 The mean MBW_{area} for the three species in the Planier sediment trap are $4.29 \mu\text{g}$ (\pm
571 $0.45 \mu\text{g}$ for *G. bulloides*, $4.04 \mu\text{g}$ ($\pm 0.4 \mu\text{g}$) for *N. incompta* and $23.25 \mu\text{g}$ ($\pm 6.2 \mu\text{g}$)
572 for *G. truncatulinoides*. The seasonal variations in shell calcification differ according
573 to the species.

574 In the case of *G. bulloides*, maximum annual calcification values are reached during
575 winter and early spring: 5.05 in December and $5.02 \mu\text{g}$ in March. January displays
576 the highest mean value: $4.78 \mu\text{g}$. Minimum values are reached during summer: 3.72
577 μg in June, which is also the month that exhibits the lowest mean MBW_{area} . Overall,
578 there is a $1 \mu\text{g}$ seasonal difference in calcification between maximum and minimum
579 values, which corresponds to a 24.5% change in the mean MBW_{area} value. Mean
580 seasonal standard deviation is $\pm 0.47 \mu\text{g}$.

581 *N. incompta* shows a maximum in calcification in late spring to mid-summer: a
582 maximum value of $5 \mu\text{g}$ is reached in May, while July is the month that displays the
583 highest mean value ($5 \mu\text{g}$). Lowest values are reached in early spring: $2.96 \mu\text{g}$ in
584 March, while January displays the lowest mean value ($3.85 \mu\text{g}$). Thus, the annual
585 mean seasonal amplitude is $1.15 \mu\text{g}$ which translates into a 28% seasonal MBW_{area}
586 variability. Standard deviation is $\pm 0.28 \mu\text{g}$.

587 Finally, *G. truncatulinoides* displays a seasonal maximum MBW_{area} value in late
588 summer-autumn, with a maximum reached in October: $35.07 \mu\text{g}$, while November;
589 is the month that shows the highest mean MBW_{area} value ($32.85 \mu\text{g}$). The lowest
590 value is reached in March: $13.57 \mu\text{g}$, and April is the month that shows the lowest
591 mean value: $18.45 \mu\text{g}$. Seasonal MBW_{area} difference is $14.3 \mu\text{g}$: a 60% variability.
592 Mean typical seasonal deviation is $\pm 3.7 \mu\text{g}$.

593

594 **4.3. Interannual MBW_{area} trends**

595 Trends throughout the 12-year record are represented in Figs. 3 and 5. In order to
596 obtain representative data for each year, maximize data availability of each species
597 and avoid the impact of months with insufficient specimens on the interannual trends,
598 only MBWs from the productive period (January to May) of each year analyzed were
599 included.

600 *G. bulloides* MBW_{area} showed a slight decrease from 1994 to 2000 and a slight
601 increase from 2000 to 2006. Over the studied interval, the lowest value is reached
602 in the year 2000 and the highest in 2004. Lowest mean annual values were reached
603 during years 2000 and 2005 (3.9 and $3.85 \mu\text{g}$, respectively).

604 On the other hand, *N. incompta* MBW_{area} showed a slight calcification reduction with
605 the highest variability in recent years. Both maximum and minimum values are

606 displayed in recent years: 2004 and 2005 respectively. Mean yearly MBW_{area} values
607 reach a maximum in 2003 (4.4 µg) and a minimum in 2005 (3.2 µg).

608 Finally, *G. truncatulinoides* MBW_{area} displayed a different pattern, with an overall
609 steep calcification increase throughout the record. Minimum calcification values are
610 observed in 1996, which is also the year with the lowest mean MBW_{area} (16.5 µg)
611 observed. Maximum value is displayed in 2003, and its mean value is also the
612 highest of the record (26.1 µg).

613 All environmental parameters showed variations across the years. Sea Surface
614 Temperatures (SSTs) displayed a slight but constant decrease over the years, while
615 salinity showed a slight increase, mainly since 2002. From late 2000 until late 2002,
616 phosphate and nitrate concentrations were exceptionally low (Fig. 5). This feature
617 has already been described in the Gulf of Lions (Meier et al., 2014). Between the 2
618 periods for which direct *in situ* carbonate system parameters measurements were
619 available, 1998 to 2000 and 2003 to 2005 (Fig. 5), CO₃²⁻ dropped by 10-15 µmol/kg,
620 DIC increased by 40 to 60 µmol/kg, leading to a pH decrease of 0.02 to 0.025.

621

622 **4.4. Sediment trap, core tops and sediment cores MBW patterns**

623 Foraminifera weights analyzed in core tops and sediment cores from the NW part of
624 the Mediterranean (Fig. 6) and radiocarbon dating allowed a further insight on
625 foraminifera calcification during the Holocene.

626 Flux-weighted MBWs (see section 3.4) from Planier sediment trap for the three
627 planktic species were 4.1 µg for *G. bulloides*, 3.9 µg for *N. incompta* and 22.3 µg for
628 *G. truncatulinoides* (Fig. 6).

629 Data from Planier core-top showed higher mean MBW_{area} values: 5.3 µg, 4.65 µg
630 and 35.4 µg. ¹⁴C dating carried out in this core-top was out of the calibration range
631 (see section 3.7 for more details), implying that this sample could be considered
632 post-industrial. Compared to the flux-weighted MBWs from the sediment trap, *G.*
633 *bulloides* weight has been reduced by 1.2 µg, *N. incompta* by 0.75 µg and *G.*
634 *truncatulinoides* by 12-13 µg.

635 Located west of Planier site, Lacaze Duthiers sediment core mean MBWs were:
636 4.99 µg for *G. bulloides*, 4.14 µg for *N. incompta*, and 32.9 µg for *G. truncatulinoides*.
637 ¹⁴C analysis displayed a post-industrial age (see section 3.7) for this sample and
638 corresponding MBWs from this sample for *G. bulloides*, *N. incompta* and *G.*
639 *truncatulinoides* respectively were: 4.7 µg, 4.3 µg and 34 µg. Overall, compared to
640 the data from the sediment trap, this corresponds to a 0.6 µg weight loss for *G.*
641 *bulloides*, 0.4 µg for *N. incompta* and 12.2 µg for *G. truncatulinoides* in.

642 Finally, in the Gulf of Minorca, northwest of Planier site, Minorca sediment core mean
643 MBWs were: 5.4 µg for *G. bulloides*, 4.5 µg for *N. incompta* and 36.3 µg for *G.*

644 *truncatulinoides* (Fig. 6). ¹⁴C dating on this core top was carried out on an
 645 intermediate depth (see section 3.7) due to the lack of availability of enough
 646 specimens in the core-top and displayed a date of 1560 calendar years BP (Table
 647 1). Corresponding MBWs for this sample were 5.4 µg, 4.9 µg, 38.2 µg for the three
 648 species. Therefore, the weight reduction compared to the sediment trap flux-
 649 weighted MBWs are: 1.3 µg for *G. bulloides*, 1 µg for *N. incompta* and finally, 16 µg
 650 for *G. truncatulinoides*.

651 **Table 4.** Mann-Whitney variance test results between the MBW_{area} of the
 652 different sites for the three species. Significant values (p<0.05) are set in bold.

		PLA ST	PLA CT	LCD SC	MR 3.1.A
		MBW _{area}			
<i>G. bulloides</i>					
PLA ST	MBW _{area}		0.110	0.003	7.86e⁻¹³
PLA CT		0.110		1	1
LCD SC		0.003	1		0.114
MIN SC		7.86e⁻¹⁴	1	0.114	
<i>N. incompta</i>					
PLA ST	MBW _{area}		0.438	0.890	2.59e⁻⁵
PLA CT		0.438		0.342	1
LCD SC		0.890	0.342		0.034
MIN SC		2.59e⁻⁵	1	0.03	
<i>G. truncatulinoides</i>					
PLA ST	MBW _{area}		0.120	0.003	3.13e⁻¹⁵
PLA CT		0.120		0.644	1
LCD SC		0.003	0.644		0.01316
MIN SC		3.13e⁻¹⁵	1	0.013	

653
 654 A Mann-Whitney variance test (see section 3.6) was carried out in order to analyze
 655 the variance between the different MBW_{area} datasets (Table 4) from the different
 656 sites. MBW_{area} data from the sediment trap appeared to have a significantly different
 657 variance compared to the MBW_{area} from Menorca sediment core for the three
 658 species ($3.13e^{-15} < p < 2.59e^{-5}$), however, differences between the sediment trap data
 659 and the with Lacaze-Duthiers sediment core were only significant for *G. bulloides*
 660 and *G. truncatulinoides* (p= 0.003). Concerning differences between the Planier
 661 sediment trap and the underlying core-top, no significant differences were observed
 662 for any of the species ($0.11 < p < 0.438$), most likely due to the small number of

663 samples from the latter site: only 2 samples were available. Note that the differences
664 between the sediment cores MBW_{area} datasets differed according to the site and
665 species. In the case of *G. bulloides*, no significant differences were observed
666 between Planier core-top, Lacaze-Duthiers sediment core and Menorca sediment
667 core. In the case of *N. incompta* and *G. truncatulinoides*, differences between
668 Lacaze-Duthiers and Menorca sediment core are significant ($0.013 < p < 0.03$),
669 although on lower orders of magnitude compared to the differences between the
670 sediment trap and sediment cores datasets (Table 4). This demonstrates that the
671 difference between the sediment trap MBW_{area} dataset and the seabed sediments
672 MBW_{area} datasets was greater than the difference between the different seabed
673 MBW_{area} datasets.

674 5. Discussion

675

676 5.1. Seasonal controls on planktic foraminifera shell calcification in the NW 677 Mediterranean

678 As described in section 4.2, the seasonal variability of MBW_{area} displays important
679 differences across the three species analyzed. The different seasonal pattern in
680 MBW_{area} is reflected by the lack of correlation between the seasonal patterns of
681 MBW_{area} of the different species, i.e., $r = -0.23$ ($p > 0.05$) between *G. bulloides* and *N.*
682 *incompta* and $r = 0.16$ ($p > 0.05$) between *G. bulloides* and *G. truncatulinoides*. Only
683 the seasonality of *N. incompta* MBW_{area} and *G. truncatulinoides* MBW_{area} share some
684 similarities, as reflected in the significant and positive correlation ($r = 0.66$; $p < 0.05$).
685 In order to examine the main controls on foraminifera seasonal calcification in the
686 Gulf of Lions, here we compare the seasonal variability of planktic foraminifera
687 calcification with foraminifera fluxes previously estimated for the Planier sediment
688 trap (Rigual-Hernández et al., 2012) satellite data for the studied site and a suite of
689 environmental parameters measured at the DYFAMED site (see section 3.4).
690 Furthermore, GAM have been generated for all three species (see Supplementary
691 figs. 3,4 and 5) and the environmental parameters considered here in order to give
692 a further insight on the potential factors controlling the MBW_{area}. These models
693 showed that *G. bulloides* and *G. truncatulinoides* seasonal calcification trends are
694 significant ($p = 0.05$ and $p = 2.4e^{-5}$ respectively). On the other hand, *N. incompta*
695 seasonal trend does not appear to be significant ($p = 0.14$).

696 **Table 5.** Correlation matrix of seasonal (monthly) test weights and the
697 environmental parameters from Planier (sediment trap and satellite data) and
698 DYFAMED site (see section 3.4). Significant correlations ($p < 0.05$) are set in
699 bold.

Parameters	Planier site data						DYFAMED site data							
	<i>G. bull.</i>	<i>N. inc.</i>	<i>G. truncat.</i>	<i>G. bull.</i>	<i>N. inc.</i>	<i>G. truncat.</i>	Chl-a	SST	Salinity	[NO ₃]	[PO ₄]	pH	[CO ₃]	[CO ₂]
	MBW _{area}			Fluxes										
<i>G. bull.</i>	1	0.232	0.167	0.012	0.027	0.152	0.318	-0.32	-0.163	0.292	0.33	0.096	0.189	0.243
<i>N. inc.</i>	-0.232	1	0.667	-0.582	-0.407	-0.405	-0.484	0.688	0.368	0.272	0.235	-0.35	0.474	-0.28
<i>G. truncat.</i>	0.167	0.667	1	-0.905	-0.725	-0.666	-0.585	0.672	-0.299	0.258	0.512	0.113	0.732	0.541

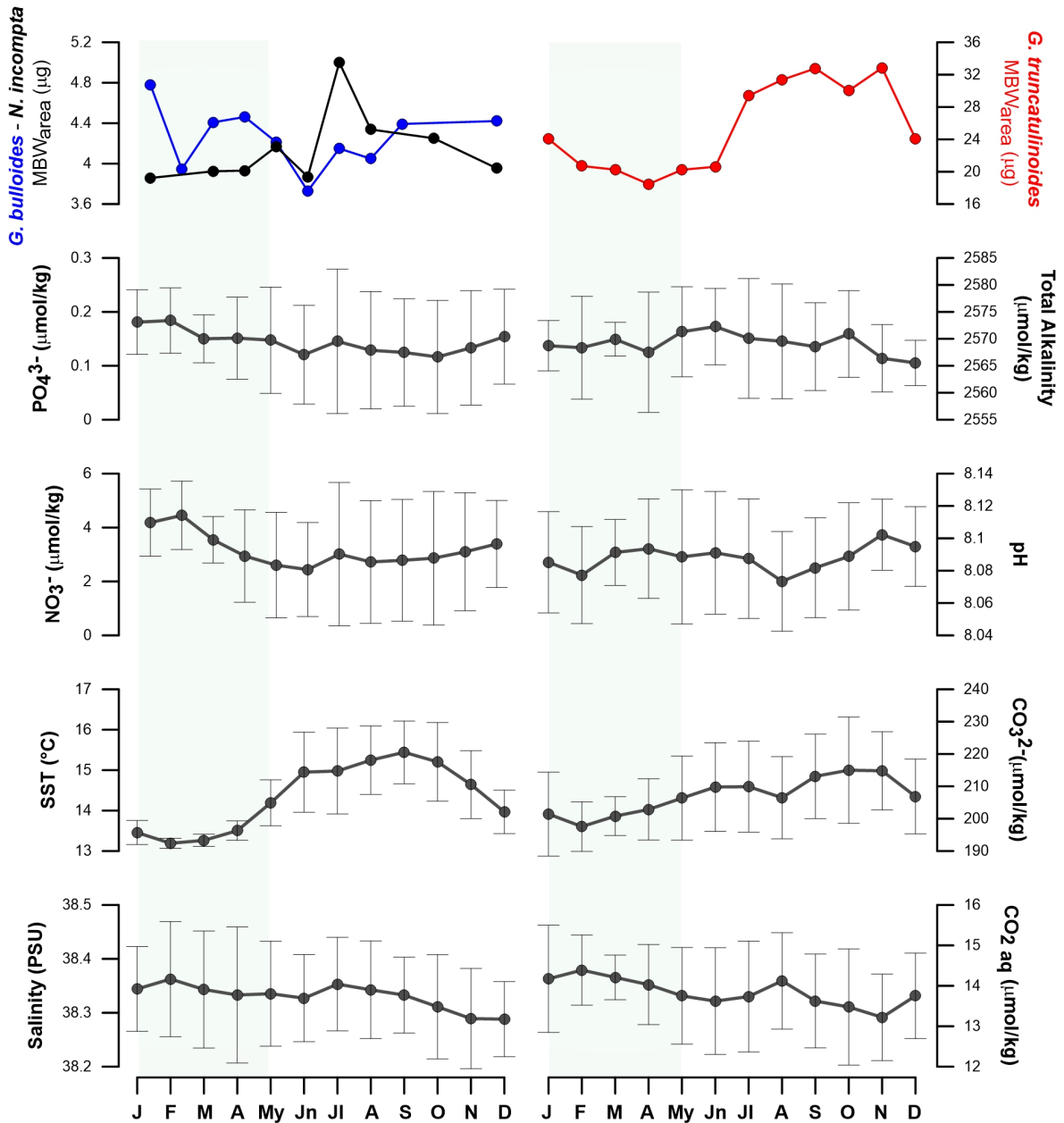
701

702 Here, we first approach seasonal shell calcification by considering the Optimum
703 Growth Conditions (OGC). Previous studies have defined these conditions on a wide
704 variety of ways: abundance of foraminifera, the chlorophyll-a concentration and even
705 nutrients concentration (de Villiers, 2004; Schiebel et al., 2001; Schiebel and
706 Hemleben, 2017). Therefore, we aim to explore the impact of these parameters as
707 OGC on the shell calcification.

708 Among all the environmental parameters, de Villiers; (2004) suggested that shell
709 calcification, and therefore MBWs, is primarily controlled by the OGC that can be
710 defined as the most suitable environmental conditions for the development of a given
711 planktic foraminifera species. Based on the latter study, it could be expected that
712 favorable environmental conditions for foraminifera growth would lead to both
713 greater shell fluxes and enhanced shell calcification. Our correlation analysis shows
714 that only *G. truncatulinoides* displays a significant (and negative) correlation with its
715 flux ($r = -0.66$, $p > 0.05$). GAM results (see Supplementary figs. 3, 4 and 5) support
716 these observations, with shell flux showing a stronger effect on the calcification for
717 *G. truncatulinoides* compared to the other two species fluxes.

718 According to the OGC theory, species calcification patterns vary according to the
719 species and their fluxes. Interestingly, *G. truncatulinoides* calcification correlates
720 negatively and significantly with all three species fluxes, a pattern opposite to what
721 the OGC theory predicts (de Villiers, 2004), i.e., optimum ecological niche is
722 associated with enhanced calcification. Thus, a possible explanation reconciling our
723 observations with the OGC theory may be that *G. truncatulinoides* tends to prioritize
724 energy allocation toward growth and reproduction at the price of a reduced
725 calcification. It is thought to reproduce once a year in winter in subtropical waters
726 and it has been speculated that nutrient availability and the lack of predation could
727 explain this strategy. During this interval, the other major species display low
728 abundances in the water column, which could allow *G. truncatulinoides* to reproduce
729 due to the lack of competition. *N. incompta* calcification displays a similar pattern, a
730 negative correlation with all three species, but with a lower level of significance. Its
731 MBW_{area} correlates negatively and significantly ($p < 0.05$) with *G. bulloides* flux, but

732 its fluxes correlate positively and significantly with the latter species fluxes (see
733 Supplementary table 2). This is interesting, as it may highlight interspecific relations.
734 First, this could lead to the assumption that when *G. bulloides* dominates the
735 assemblages, *N. incompta* also displays a high abundance (Rigual-Hernández et
736 al., 2012). Then, it could show that when conditions are favorable, *N. incompta*
737 reproduces at a higher rate at the price of thinner shells (Table 1). This agrees with
738 *N. incompta* life cycle, which is known to be outnumbered by opportunistic species
739 when nutrients supply is high (Schiebel et al., 2002), but dominate the assemblages
740 when stratified waters are set, therefore, when conditions are favorable or when in
741 cohabitation with opportunistic species, it could focus on its reproduction. Note that
742 *G. truncatulinoides* and *N. incompta* MBW_{area} correlate positively and significantly
743 ($p < 0.05$), showing a similar calcification pattern on a seasonal scale.
744 An alternative proxy for OGC that may be considered is chlorophyll-a concentration.
745 Chlorophyll is considered an indicator of the algal biomass concentration, which is
746 known to represent a large part of some foraminifera species diet (Schiebel and
747 Hemleben, 2017). However, our data only showed a significant correlation of
748 chlorophyll-a with *G. truncatulinoides* calcification. A stronger trend would be
749 expected under the OGC theory for *G. bulloides* as algae are a vital part of its diet
750 (Hemleben et al., 1989; Schiebel and Hemleben, 2017). This lack of correlation
751 between *G. bulloides* and chlorophyll-a has already been described (Weinkauff et al.,
752 2016). We speculate that *G. bulloides* may preferentially feed on certain groups of
753 phytoplankton which changes in seasonal abundance in the photic zone do not
754 necessarily follow the seasonal pattern of total chlorophyll concentration (Marty et
755 al., 2002). Also, note that the chlorophyll-a data presented here only represents the
756 conditions in the surface layer. GAM results further support these observations (see
757 Supplementary fig. 5), with chlorophyll-a showing a significant impact on *G.*
758 *truncatulinoides* calcification. This observation indicates that optimum calcification
759 conditions for *G. truncatulinoides* are reached at times of minimum annual algal
760 biomass concentration in the photic zone. It is possible that, due to its deeper habitat
761 (Schiebel and Hemleben, 2017), *G. truncatulinoides* feeds on phytoplankton
762 dwelling in subsurface levels of the water column. In fact, a deep chlorophyll
763 maximum is known to develop during large part of the year in the Northwestern
764 Mediterranean (Estrada et al., 1993) but its presence is not detected by satellites.
765 This interpretation is in agreement with earlier work by Pujol and Vergnaud Grazzini,
766 (1995) who found peak abundances of this species during the summer below the
767 thermocline.



768

769

770

771

772

Figure 4. *G. bulloides*, *N. incompta* and *G. truncatulinoides* seasonal mean monthly MBW_{area} variations compared with Planier environmental data and the resampled seasonal signal of environmental parameters from the DYFAMED site across a composite year.

773

774

775

776

777

778

Previous studies have described that, in those settings where foraminifera abundance covaries with nutrient concentrations, then nutrients are probably a better OGC proxy than chlorophyll concentrations (Schiebel et al., 2001). In turn, the correlation of nutrients (nitrates and phosphates) with fluxes were positive for all three species, although only significant ($p < 0.05$) for *G. truncatulinoides* abundance ($r = 0.58$ and 0.59 for nitrates and phosphates respectively). Although here we have

779 first described the OGC as species fluxes and then as the chlorophyll-a
780 concentration, it is important to remember that the niche and favorable conditions
781 meant to be described by the OGC for each species are multi-dimensional.

782 Note that nitrate and phosphate concentration variations were closely linked to each
783 other ($r= 0.876$, $p<0.05$), making it difficult to determine if the resulting effect on
784 foraminifera calcification is due to the effect of a single driver or to the combination
785 of both. Our work shows that nutrient concentrations (both nitrates and phosphates)
786 do not correlate significantly with any of the three species MBW studied, and this
787 observation is supported by the GAM results which do not show any significant effect
788 of nutrients concentrations on the calcification.

789 Previous studies have suggested that salinity may have an influence on foraminifera
790 calcification (Zarkogiannis et al., 2022). However, our data suggest that the role of
791 salinity on calcification in our study region is unlikely since its seasonal amplitude is
792 tiny (0.1 PSU; Fig. 4). This idea is supported by the lack of correlation between
793 salinity and MBW_{area} for the three species studied (Table 5) and the GAM results.

794 Temperature (Sea Surface Temperature) has been described as a major factor that
795 controls the size (Schmidt et al., 2004) and porosity (Burke et al., 2018) of planktic
796 foraminifera, therefore it could represent a major control factor on shell calcification
797 in the NW Mediterranean. In particular, calcification could be positively linked to
798 temperature through different mechanisms: (i) warmer temperatures have been
799 shown to increase enzymatic activity and therefore enhanced growth and
800 calcification rates (Spero et al., 1991); (ii) Lombard et al., (2011) stated that higher
801 temperatures could also increase feeding and ingestion rates, but it remains unclear
802 if this could result in a calcification rate increase. Our data revealed that SST
803 correlates positively and significantly with *N. incompta* and *G. truncatulinoides*
804 calcification ($r= 0.69$ and 0.67 respectively, $p<0.05$). GAM results also displayed a
805 positive and the most significant effect of the SST on these two species. These
806 findings highlight that SSTs are one of the main factors affecting *N. incompta* and *G.*
807 *truncatulinoides* calcification among the parameters considered here. Finally, in
808 addition to having an impact on the size and calcification of the planktic foraminifera,
809 temperature is well known as a major control of the carbonate system, due to the
810 increased solubility of atmospheric CO₂ at lower temperatures, and therefore it could
811 have an indirect effect on foraminifera calcification by affecting the carbonate
812 system.

813 Data for the carbonate system were only available for years 1998 to 2000 and 2003
814 to 2005 and, therefore gaps comprised in these years were filled with estimates
815 using the CO2sys macro (see section 3.6 for more details). However, note that the
816 data available for these parameters was relatively smaller compared to the other
817 parameters and may have prevented detection of other significant relationships. The

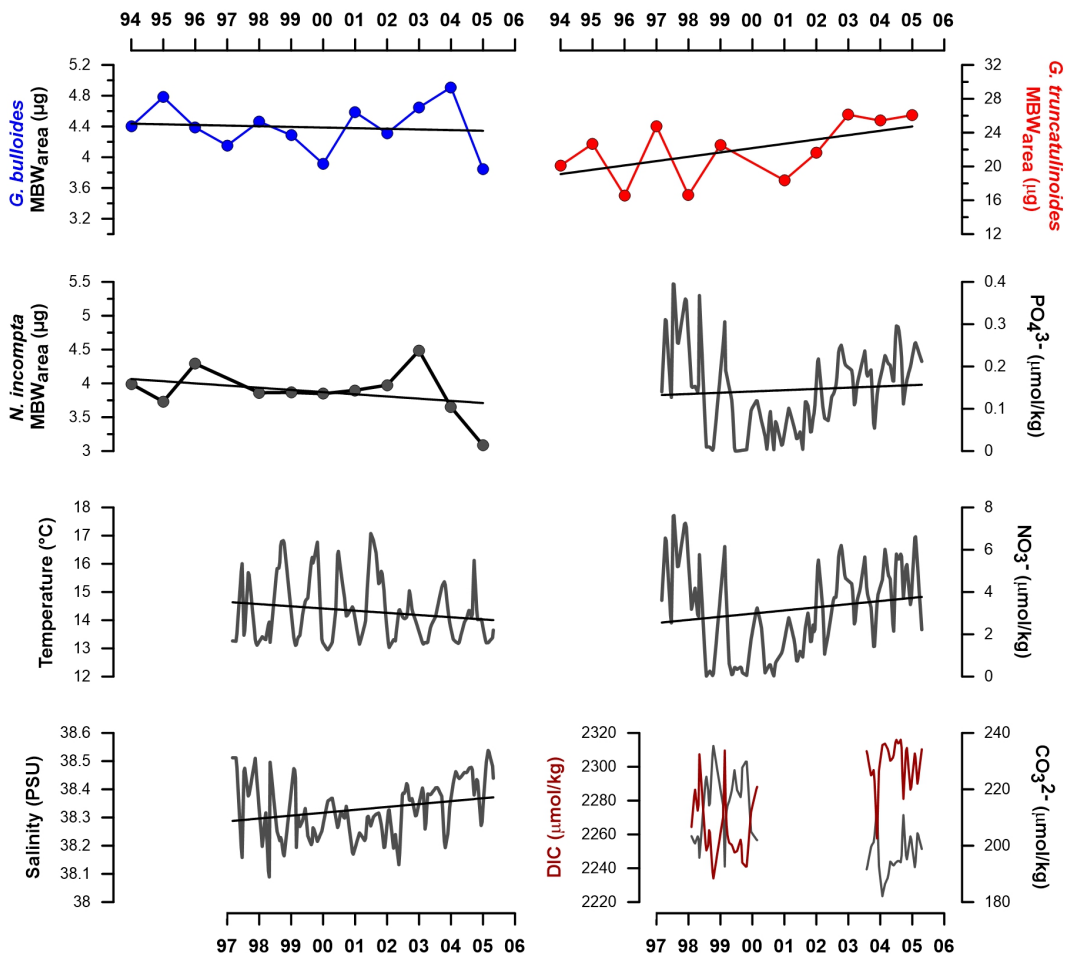
818 relationship between CO_3^{2-} and MBW has been described in previous studies
819 (Barker and Elderfield, 2002; Marshall et al., 2013) and the bulk of evidence indicates
820 that foraminifera MBWs to be positively linked with CO_3^{2-} concentrations (Aldridge et
821 al., 2012; Osborne et al., 2016). However, it appeared that planktic foraminifera
822 response to CO_3^{2-} concentration was not uniform and varied across species (Beer
823 et al., 2010; Lombard et al., 2010). The trends between carbonate system
824 parameters and MBWs were similar to those observed when comparing MBWs with
825 temperature, highlighting the covariations between these two parameters (Fig. 4).
826 Our data showed that CO_3^{2-} concentrations were only significantly correlated with *G.*
827 *truncatulinoides* MBW_{area} ($r= 0.73$, $p<0.05$), implying that carbonate availability may
828 represent a key control on this species in the Northwestern Mediterranean. On the
829 other hand, GAM result (see Supplementary figs. 3, 4 and 5) did not show a
830 significant impact of any carbonate system parameters for any of the three species
831 calcification. As stated previously, the lack of data could have prevented the
832 detection of further trends, but considering the seasonal patterns of carbonate
833 system parameters, a potential role of the CO_3^{2-} concentration could be expected.
834 In summary, seasonal correlations, trends and GAM showed that the environmental
835 parameters that displayed the highest correlation with MBW_{area} vary according to the
836 species. *G. bulloides* calcification appeared to be affected mainly by the OGC and
837 interspecific relations. *N. incompta* calcification showed to be mainly positively linked
838 to the SST. Finally, *G. truncatulinoides* calcification was positively linked with the
839 SST and potentially CO_3^{2-} concentration, while OGC displayed a negative effect on
840 its MBW_{area} . The combined effect of these parameters seems to control foraminifera
841 calcification in the Gulf of Lions; however, it should be considered that covariation
842 between these parameters is strong, and therefore it is difficult to isolate the effect
843 of a single parameter. Moreover, it is likely that the ecology and life cycle of the
844 species could also be a major factor affecting the response of the species
845 calcification to the environmental parameters variations. Our results are in
846 agreement with earlier studies that stated that OGC (de Villiers, 2004), SST and
847 CO_3^{2-} (de Villiers, 2004; Marshall et al., 2013; Osborne et al., 2016) concentrations
848 are the main factors that impact calcification in planktic foraminifera, while the
849 calcification response to those parameters is species-specific, which is in agreement
850 with the work of Weinkauf et al, (2016).

851

852 **5.2. Interannual trends in planktic foraminifera calcification**

853 As stated previously, the Mediterranean Sea is a sensitive zone to atmospheric CO_2
854 accumulation (Ziveri, 2012) and is experiencing ongoing ocean acidification. On an
855 interannual time scale, different studies (Beer et al., 2010; Osborne et al., 2016)
856 have shown that sea surface warming and carbonate system parameters are the

857 most likely parameters to control calcification on key calcifying phytoplankton
 858 species such as the coccolithophore *Emiliana huxleyi* organisms (Meier et al.,
 859 2014). However, datasets from sediment traps that cover a wide span of years and
 860 in which foraminifera weights have been analyzed are rare (Kiss et al., 2021),
 861 therefore it is difficult to place our results in a more global context. Our GAM results
 862 (see Supplementary figs. 3 and 4) showed that both *G. bulloides* and *N. incompta*
 863 interannual patterns were non-significant. This is not surprising as the calcification
 864 trends for these two species did not display a clear and marked variation over the
 865 years, excepting a small mean calcification reduction (Fig. 3) and minimum
 866 calcification values in 2004 and 2005 (Fig. 3 and Supplementary figs. 3 and 4).
 867



868

869 **Figure 5.** Interannual mean MBW_{area} (µg) values for *G. bulloides*, *N. incompta*
 870 and *G. truncatulinoides* from the high productivity period (see section 2) and
 871 Planier and DYFAMED environmental data variations across the record.
 872 Black lines represent the trends from the MBW_{area} and resampled data. DIC
 873 represents “Dissolved Inorganic Carbon”.

874 Notably, the trend in *G. truncatulinoides* is opposed to the previous two species and
875 shows a steady and steep increase throughout our record. Over the analyzed time
876 span, its MBW increased around 20% (equivalent to an increase of ~5 µg).
877 According to the GAM results, the interannual calcification trend for this species is
878 significant (see Supplementary fig. 5). If this calcification increase continues on
879 current trends, then the average MBW of *G. truncatulinoides* will double by 2024.
880 Analysis of present *G. truncatulinoides* populations is urgently needed to assess if
881 the observed trend held true during the last two decades. It is important to note that
882 while *G. truncatulinoides* seems to exhibit a positive correlation with CO₃²⁻
883 concentration on a seasonal scale, no clear correlation was found with the
884 interannual changes of CO₃²⁻ concentration. This feature is also supported by the
885 GAM results. A similar enhancement in shell calcification has been described in the
886 Balearic Sea for *G. truncatulinoides* in high-resolution sediment cores (Pallacks et
887 al., 2020), but also in *Globorotalia inflata*. Taken together, our observations and the
888 study mentioned above, suggest that deep dwellers are unaffected by the recent
889 ocean acidification and changes in the carbonate system and that the recent change
890 in one or several environmental drivers may be stimulating the calcification of these
891 species.

892 Here, we theorize that the interannual patterns presented in Figs. 3 and 5 mainly
893 reflect the seasonal changes in the regional oceanographic setting. As described
894 previously (see section 2 for more details), the Gulf of Lions is influenced by a strong
895 seasonality. The recent SST decrease could be linked to an enhancement in water
896 mixing, as cold and deep salty water reach up to the surface. This mechanism would
897 be less intense during years 2000 to 2002, corresponding to a SST increase along
898 with a salinity decrease and absolute minimums in nutrients concentrations (Fig. 5),
899 as water stratifies, these are consumed by primary production. Finally, in recent
900 years, water mixing seems to be reactivated, as SST keeps decreasing and nutrients
901 concentrations increase again. This mechanism also affects the carbonate system
902 parameters, as water mixing brings to surface deeper DIC enriched waters to the
903 surface, coupled with a [CO₃²⁻] reduction. Our data shows that alkalinity patterns
904 display similar tendencies to DIC, however, until the second time span covered by
905 carbonate system data, alkalinity variations are proportionally higher than DIC
906 variations (see Supplementary material), suggesting a water mixing phenomenon.
907 On the other hand, DIC variations turn to be higher than alkalinity variations from
908 2003 to 2005, suggesting an additional effect of carbon inputs on the carbonate
909 system not reflected in the alkalinity data.

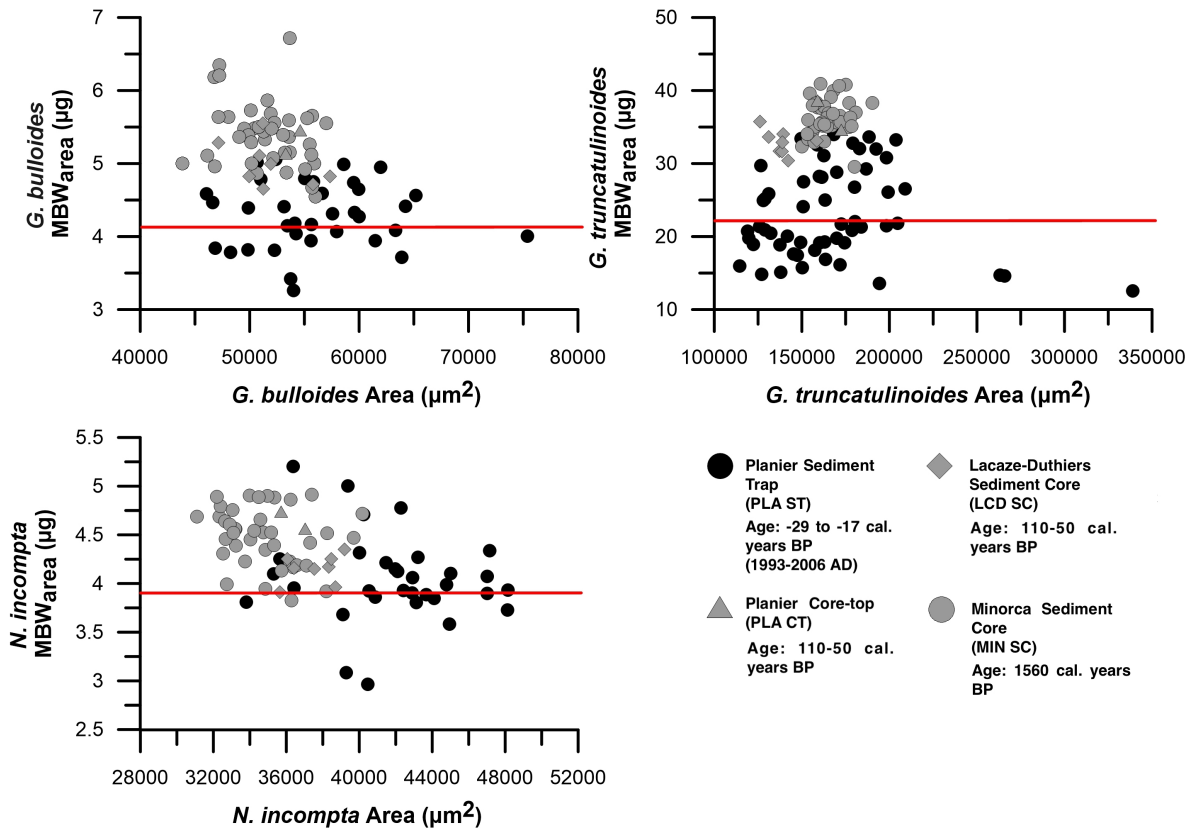
910 Note that SSTs, despite showing a positive and significant correlation with *N.*
911 *incompta* and *G. truncatulinoides* on a seasonal scale and the GAM showing a
912 positive and significant effect on the calcification, did not follow the same pattern as

913 the latter species. This observation implies that other mechanisms or parameters
 914 than the ones considered here may be affecting the MBW_{area} on recent years.

915

916 **5.3. Holocene core-top data comparison**

917



918

919

920

921

922

923

924

925

Figure 6. MBW_{area} in μg and area in μm^2 comparison in the sediment trap (PLA ST), Planier core-top (PLA CT), and both Lacaze-Duthiers (LCD SC) and Minorca sediment core (MR 3.1.A). Black dots represent data from the sediment trap, while lighter colors represent data from the different seabed sediments. Red lines represent the flux-weighted values from the sediment trap. Note that the age provided represent the dating (see section 3.7) results carried out in specific samples of each site (see section 4.3).

926

927

928

929

930

931

932

933

934

The comparison of the well-preserved assemblages of planktic foraminifera in the pre-industrial and industrial Holocene-aged surface sediments with those collected by a long-sediment trap record offers a unique opportunity to assess the impact of recent environmental change on the calcification of calcareous zooplankton in the Mediterranean Sea (Fig. 6). However, when comparing data from sediment traps and seabed sediments, the possible role of calcite dissolution must be taken into account.

Calcite dissolution in the water column and/or on the sea floor could be invoked as a source of variability between the sediment trap and surface sediment data sets

935 (e.g., Dittert et al., 1999). Therefore, in order to obtain meaningful interpretations
936 from our data sets it is important to assess the possible role of dissolution in the
937 preservation of planktic foraminifera shells. Several lines of evidence suggest,
938 however, that calcite preservation does not represent an important source of bias in
939 our study area. Firstly, the Mediterranean Sea is supersaturated with respect to
940 calcite (Millero et al., 1979) and the location of all the analyzed samples is much
941 shallower than the location of the calcite saturation horizon (Álvarez et al., 2014),
942 therefore, calcite dissolution seems unlikely (Schneider et al., 2007). Secondly,
943 several sediment trap studies have documented that calcareous plankton
944 experience negligible dissolution in their transit from the surface ocean to the sea
945 floor (Beaufort et al., 2007; Moy et al., 2009; Rigual-Hernández et al., 2020). Thirdly,
946 SEM and microscopic observations of all 3 species in samples from both the
947 sediment traps and sediment cores showed no sign of dissolution and foraminifera
948 were well preserved (see Supplementary fig. 6). These arguments suggest that
949 calcite dissolution does not represent an important control in the weight of the
950 planktic foraminifer shells in the analyzed samples. However, it has been
951 documented that when dissolution takes place, the thinnest shells are affected first
952 (Berger, 1970) while the heaviest and more calcified specimens remain. In our study,
953 the specimens from the sediment trap were lighter than the ones from the sediment
954 cores, which corresponds to the previous statement. This is important to
955 acknowledge as the individuals from the seabed sediment could only represent more
956 calcified and solid individuals, while the most fragile and less calcified individuals
957 may not have been preserved. Therefore dissolution cannot be completely ruled out
958 here as a possible source of variability between the surface sediment and sediment
959 trap data sets.

960 Overall, the lower shell weights of the foraminifera collected by the traps suggests
961 that the three planktic foraminifera species may have experienced a reduction in
962 their calcification since pre-industrial times to post-industrial and recent Holocene.
963 While the shell weight of each species measured in the sediments show some
964 variability across seabed sediments (Fig. 6), our data suggest an overall reduction
965 of 18-24% for *G. bulloides*, 9-18% for *N. incompta*, and 32-40% for *G.*
966 *truncatulinoides*. It is important to note that the range of shell weight variability across
967 core-tops and sediment cores (4.5-6.7 μg and 0.37 μg typical deviation for *G.*
968 *bulloides*, 3.8-4.9 μg and 0.23 μg typical deviation for *N.incompta*, and 29.5-40.9 μg
969 and 2.6 μg typical deviation for *G. truncatulinoides*) is substantially lower than the
970 difference with the sediment trap data (3-5 μg and 0.5 μg typical deviation for *G.*
971 *bulloides*, 2.9-5.2 μg and 0.5 μg typical deviation for *N. incompta* and 12-35 μg and
972 6 μg typical deviation for *G. truncatulinoides*), implying that the shell weight of recent
973 foraminifera populations for the three species is lower than anywhere in the NW

974 Mediterranean in the pre-industrial and post-industrial times. The source of the
975 variability across core tops and sediment cores is most likely caused by the different
976 age of the samples, ranging from 1560 cal. years BP at Minorca mid-depth (Table
977 1) sample to post-industrial at Planier and Lacaze-Duthiers core-tops, and the
978 different environments associated to the location of each core top.

979 A non-parametric two-way Mann-Whitney test (see sections 3.6 and 4.3) showed
980 that the sediment trap MBW_{area} dataset was significantly different ($p < 0.05$) from MR
981 3.1.A and non-different from PLA CT for all three species studied here (Table 5).

982 Something to consider when comparing recent sediment trap data with pre-industrial
983 Holocene data is the life cycle of the species. As all the species analyzed presented
984 a lighter weight in the sediment traps, the degree to which the different specimens
985 responded vary. The greatest weight reductions were observed for *G.*
986 *truncatulinooides* populations, while *N. incompta* populations exhibited the lowest
987 weight loss.

988 Previous work stated that those species hosting photosynthetic algal symbionts
989 exhibit a higher tolerance to environmental changes that may affect their calcification
990 (Lombard et al., 2009). This is due to the fact that these symbionts can modify the
991 sea water chemistry that is in a close range to the shell, allowing a calcification
992 enhancement. Of the species studied here, none are known, with the possible
993 exception of *G. bulloides*, to be symbiont bearing species, therefore, they are among
994 the most vulnerable foraminifera species to any sea water chemistry change.

995 It has been described that some morphotypes of *G. bulloides* host bacterial
996 endobionts in their cytoplasm (Bird et al., 2017). The later work showed that high
997 amounts of *Synechococcus*, a cyanobacteria, were found in morphotype Id
998 specimens of *G. bulloides* from the California coast. Although no such observations
999 have been reported on morphotype Ib, the dominant *G. bulloides* morphotype in the
1000 Mediterranean sea (Schiebel and Hemleben, 2017), this could be relevant as
1001 bacterial photosynthetic activity would interact on the close range seawater
1002 chemistry by removing $^{12}\text{CO}_2$ and therefore impacting the $^{13}\text{C}/^{12}\text{C}$ ratios in the
1003 surrounding dissolved CO_2 . Moy et al., (2009) work in the Southern Ocean, showed
1004 a 30-35% calcification reduction for *G. bulloides* during the industrial era. Our study
1005 shows that such a similar reduction in *G. bulloides* MBW_{area} (i.e., a mean 20% taking
1006 into account the 3 sites studied) has also taken place in the Mediterranean Sea.

1007 Even though the species studied were different in Fox et al., (2020), and that shell
1008 thickness was analyzed, the latter work showed a massive shell reduction for *N.*
1009 *dutertrei* (around 75%) and a smaller reduction for *G. ruber* (around 20%). Mean *N.*
1010 *incompta* weight reduction in this study is around 15%, despite that life cycles are
1011 different between these species, our results come in the same line.

1012 Data for *G. truncatulinoides* calcification comparison between pre-industrial and
1013 post-industrial Holocene is scarce. One of the few available studies is the one of
1014 Pallacks et al., (2020) in the western Mediterranean sea using pre-industrial data
1015 and recent foraminifera weight data obtained from high resolution core-tops. *G.*
1016 *truncatulinoides* showed a 24% weight reduction, which is a lower reduction than
1017 what is shown in our study (around 35% MBW_{area} decrease), but shows a similar
1018 trend. Taken together, all these observations suggest that a decrease in major
1019 planktic foraminifera calcification is not only a regional feature but a global scale
1020 process.

1021 On a more regional scale, Hassoun et al., (2015) documented the ongoing changes
1022 in seawater carbonate speciation in the Mediterranean waters. In the latter work, the
1023 distributions of anthropogenic CO₂ showed that all Mediterranean water masses
1024 have already experienced ocean acidification. This effect was more pronounced in
1025 the intermediate to deep masses (300-500m and >500m respectively) in the western
1026 basin, which translated into a minimum pH reduction of 0.1 in this part of the
1027 Mediterranean. As stated previously, over the years in which carbonate parameters
1028 were retrieved from the DYFAMED database, pH was reduced, DIC showed a
1029 marked increase and [CO₃²⁻] displayed a decrease. Taken together these
1030 observations and our data, it is possible that the observed changes in foraminifera
1031 calcification could have been partially driven by the ongoing ocean acidification in
1032 the Mediterranean.

1033 Moreover, the largest calcification reduction is observed between the seabed
1034 sediments and the sediment trap, this means that the highest calcification reduction
1035 has taken place between post-industrial Holocene and recent Holocene (i.e. the
1036 reduction between LCD SC/PLA CT and PLA ST) (Fig. 6). This could be explained
1037 with the “Great Acceleration theory”. The Great Acceleration is a term used to
1038 describe the trends in CO₂ emissions and the associated temperature changes as
1039 consequences of the human impacts on the atmosphere since the 1950s (Head et
1040 al., 2022a, 2022b).

1041 However, other important changes in physical and chemical parameters co-occur
1042 with ocean acidification, and therefore should be also considered. Based on the
1043 seasonal and interannual patterns of the SST in the Gulf of Lions (Figs. 4 and 5),
1044 temperature trends could also be invoked as a likely parameter to affect calcification
1045 here. As shown by the correlations (Table 5) and the GAM results, SSTs are one of
1046 the most likely parameters to affect calcification on different timescales. However,
1047 on a pre-industrial to post-industrial timescale, the effect of the SST on the
1048 foraminifera calcification on longer time scales may be hard to evaluate due to the
1049 effect of the latter on the carbonate system parameters such as CO₂ and CO₃²⁻-
1050 concentration in the water. But note that the Mediterranean is considered to be

1051 warming at a faster rate than the global average (Hassoun et al., 2015; Lazzari et
1052 al., 2014).

1053 Calcification data from the sediment trap has been flux-weighted (see section 3.4) in
1054 order to be compared with the sedimentary calcification data, therefore, this data
1055 could be affected by a change in the incoming foraminifera flux (de Moel et al., 2009).
1056 In this line, the Gulf of Lions, presents a marked seasonality (see section 2) and the
1057 both the mass fluxes (Heussner et al., 2006) and foraminifera fluxes present strong
1058 seasonal variations. Parameters such as the North Atlantic Oscillation index, the
1059 river runoff and the intensity of the seasonal water cascading process have been
1060 suggested to play a role on planktic foraminifera production and export (Rigual-
1061 Hernández et al., 2012). The later study shows that most of the species flux showed
1062 a yearly uni-modal distribution, but the flux values and distribution remained fairly
1063 constant over the years. This highlights that, in our study zone, a major change in
1064 the foraminifera flux affecting the flux-weighted calcification value is unlikely.

1065 In summary, our results suggest that the interactive effect of rising ocean acidity,
1066 and enhanced SST (regionally amplified in the NW Mediterranean, (Hassoun et al.,
1067 2022, 2015)) represent the most likely responsible factors for the MBW differences
1068 between the pre-industrial and post-industrial to recent Holocene. However, the
1069 analysis of seasonal and interannual trends indicates that the influence of these
1070 parameters is species-specific and varies across the studied time scales. This
1071 implies that the controls of planktonic foraminifera are complex and that factors other
1072 than ocean acidification and warming are likely to also account for part of the
1073 variability observed between sediment trap and seabed sediments.

1074

1075 **5.4. Influence of environmental variability on MBW_{area} across different time** 1076 **scales**

1077 Our results show that the influence of environmental parameters over the different
1078 time scales studied is not constant and depends on the species, the environmental
1079 driver and timescale.

1080 In the case of *G. bulloides*, our data suggest that OGC and inter-specific
1081 relationships seem to affect its MBW on a seasonal scale, carbonate system seems
1082 to play a major role while on an interannual and on a pre/post-industrial time scales.
1083 *N. incompta* calcification seems affected by OGC, inter-specific relationships and
1084 SST on a seasonal scale, while on longer time-scales carbonate system appears to
1085 play preponderant role. Finally, *G. truncatulinoides* calcification seems positively
1086 correlated to carbonate system and SSTs and negatively with the OGC on a
1087 seasonal scale. However, these patterns seem to have an opposite effect on an
1088 interannual scale, as *G. truncatulinoides* calcification shows a clear increase while
1089 carbonate system parameters become less and less favorable for calcification. In

1090 turn, on a pre/post-industrial Holocene time scale, its MBW_{area} seem to be affected
1091 by regional processes such as OA and warming.
1092 Factors such as changes in the regional oceanographic processes (Cisneros et al.,
1093 2019; Durrieu de Madron et al., 2017) affect the physical and chemical properties of
1094 the water column and hence, could impact the life cycle of the species studied here.
1095 Also, while *G. bulloides* can either present regular or encrusted forms; *N. incompta*
1096 and *G. truncatulinoides* are crust forming species. In our study, *G. bulloides*
1097 individuals are mainly regular forms, but encrusted individuals were identified in both
1098 the sediment trap and seabed sediments. It is out of the scope of this work to focus
1099 on the effect of the crust on the species MBW, however, Osborne et al., (2016) study
1100 showed that encrusted *G. bulloides* individuals are around 20-30% heavier than the
1101 regular ones.

1102 6. Conclusions

1103

1104 The variability in shell calcification of three planktic foraminifera species (*G.*
1105 *bulloides*, *N. incompta* and *G. truncatulinoides*) was studied in the northwestern
1106 Mediterranean Sea at different time scales using sediment trap and seabed samples.
1107 The analysis of 273 samples and more than 4000 individuals revealed that:

- 1108 i. The Sieve Based Weight (SBW) method is not a reliable tool as
1109 calcification indicator due to the influence of morphometric parameters on
1110 foraminifera weight. The Measured Based Weight (MBW) technique, on
1111 the other hand, shows little to negligible influence of the morphometric
1112 parameters, and therefore, can be considered a reliable calcification
1113 proxy.
- 1114 ii. Analysis of the seasonal variability of planktic foraminifera calcification
1115 revealed important differences between species. *G. bulloides* exhibited
1116 peak calcification during winter, *N. incompta* during mid-summer and *G.*
1117 *truncatulinoides* during late summer to autumn.
- 1118 iii. Interannual analysis suggest that *G. bulloides* and *N. incompta* did not
1119 display any significant pattern between 1994 and 2005, on the other hand,
1120 *G. truncatulinoides* displays a constant and steady calcification increase
1121 over recent years.
- 1122 iv. Sediment trap and seabed sediment data comparisons between pre-
1123 industrial, post-industrial and recent Holocene assemblages showed that
1124 all three species experienced a calcification reduction. Modern *G.*
1125 *bulloides*, *N. incompta* and *G. truncatulinoides* individuals were 18-24%,
1126 9-18% and 32-40% less calcified respectively.

1127 v. Finally, correlations with environmental parameters and GAM indicate that
1128 Optimum Growth Conditions affect positively *G. bulloides* and negatively
1129 *G. truncatulinoides* calcification respectively. Sea Surface Temperatures
1130 affect positively both *N. incompta* and *G. truncatulinoides* calcification.
1131 Finally, CO_3^{2-} concentration is also a likely parameter to influence
1132 positively planktic foraminifera calcification in the Northwestern
1133 Mediterranean. However, calcification appeared to be species-specific
1134 and vary depending on the time scale studied. This may suggest that other
1135 parameters than the ones studied here may play a role in foraminifera
1136 calcification.

1137 As planktic foraminifera represent roughly about 50% of pelagic calcite production
1138 (Schiebel, 2002) in the world's oceans, and therefore, an important component of
1139 the marine carbon cycle, a reduction in the calcification of their shell could induce
1140 important changes in the future carbon cycle with feed-backs on climate. Our results
1141 call for increasing efforts in monitoring planktic foraminifera calcification the
1142 Mediterranean in order to determine if the trends suggested by our data will be
1143 sustained over time.

1144
1145 The Supplement related to this article is available at DOI: 10.17632/4t9x554dwz.1

1146
1147 *Competing interests.* The authors declare that they have no conflict of interest.

1148 *Author contributions.* ARH, FJS and TMB designed the study. JPT designed Figures 1 and
1149 2 and contributed to data discussion. XDM provided Planier core-top and Lacaze-Duthiers
1150 seabed sediment samples. IC provided the Minorca promontory seabed sediment samples.
1151 NH carried out the ^{14}C measurements. AH performed the numerical analyses and
1152 contributed to their interpretations. TMB led the sample processing as well as the
1153 microscopy and image analysis, the foraminifera study and wrote the manuscript with
1154 feedback from all authors.

1155 *Acknowledgments.* Authors would like to thank the two anonymous reviewers for their critical
1156 comments that helped improve this manuscript. Authors would also like to thank Blanca
1157 Ausín for her insight on radiocarbon dating and Serge Heussner for the retrieval of the
1158 sediment trap collected within the French MOOSE program (Mediterranean Ocean
1159 Observing System for the Environment) coordinated by CNRS-INSU and the Research
1160 Infrastructure ILICO (CNRS-IFREMER). This study was funded by the Spanish “Ministerio
1161 de Ciencia e Innovación” through a grant number PRE2019-089091 and through the project
1162 RTI2018-099489-B-100; PID2021-128322NB-100. This project has received funding from
1163 the project BASELINE (PID2021-126495NB-741 C33) granted by Spanish Ministry of
1164 Science, Innovation and Universities (ARH).

1165 References

- 1166 Aldridge, D., Beer, C. J., and Purdie, D. A.: Calcification in the planktonic foraminifera;
1167 *Globigerina bulloides*; linked to phosphate concentrations in surface waters of the North
1168 Atlantic Ocean, *Biogeosciences*, 9, 1725–1739, <https://doi.org/10.5194/bg-9-1725-2012>,
1169 2012.
- 1170 Álvarez, M., Sanleón-Bartolomé, H., Tanhua, T., Mintrop, L., Luchetta, A., Cantoni, C.,
1171 Schroeder, K., and Civitarese, G.: The CO₂ system in the Mediterranean Sea: a basin wide
1172 perspective, *Ocean Sci.*, 10, 69–92, <https://doi.org/10.5194/os-10-69-2014>, 2014.
- 1173 Azibeiro, L. A., Kučera, M., Jonkers, L., Cloke-Hayes, A., and Sierro, F. J.: Nutrients and
1174 hydrography explain the composition of recent Mediterranean planktonic foraminiferal
1175 assemblages, *Marine Micropaleontology*, 179, 102201,
1176 <https://doi.org/10.1016/j.marmicro.2022.102201>, 2023.
- 1177 Barker, S. and Elderfield, H.: Foraminiferal Calcification Response to Glacial-Interglacial
1178 Changes in Atmospheric CO₂, *Science*, 297, 833–836,
1179 <https://doi.org/10.1126/science.1072815>, 2002.
- 1180 Bé, A. W. H., Hutson, W. H., and Be, A. W. H.: Ecology of Planktonic Foraminifera and
1181 Biogeographic Patterns of Life and Fossil Assemblages in the Indian Ocean,
1182 *Micropaleontology*, 23, 369, <https://doi.org/10.2307/1485406>, 1977.
- 1183 Beaufort, L., Probert, I., and Buchet, N.: Effects of acidification and primary production on
1184 coccolith weight: Implications for carbonate transfer from the surface to the deep ocean:
1185 oceanic carbonate transfer, *Geochem. Geophys. Geosyst.*, 8, n/a-n/a,
1186 <https://doi.org/10.1029/2006GC001493>, 2007.
- 1187 Beer, C. J., Schiebel, R., and Wilson, P. A.: Technical Note: On methodologies for determining
1188 the size-normalised weight of planktic foraminifera, *Biogeosciences*, 7, 2193–2198,
1189 <https://doi.org/10.5194/bg-7-2193-2010>, 2010a.
- 1190 Beer, C. J., Schiebel, R., and Wilson, P. A.: Testing planktic foraminiferal shell weight as a
1191 surface water [CO₃²⁻] proxy using plankton net samples, *Geology*, 38, 103–106,
1192 <https://doi.org/10.1130/G30150.1>, 2010b.
- 1193 Bergamasco, A. and Malanotte-Rizzoli, P.: The circulation of the Mediterranean Sea: a
1194 historical review of experimental investigations, *Advances in Oceanography and*
1195 *Limnology*, 1, 11–28, <https://doi.org/10.1080/19475721.2010.491656>, 2010.
- 1196 Berger, W. H.: Planktonic Foraminifera: Selective solution and the lysocline, *Mar. Geol.*, 8,
1197 111–138, 1970.
- 1198 Bethoux, J. P., Gentili, B., Morin, P., Nicolas, E., Pierre, C., and Ruiz-Pino, D.: The
1199 Mediterranean Sea: a miniature ocean for climatic and environmental studies and a key for
1200 the climatic functioning of the North Atlantic, *Progress in Oceanography*, 44, 131–146,
1201 [https://doi.org/10.1016/S0079-6611\(99\)00023-3](https://doi.org/10.1016/S0079-6611(99)00023-3), 1999.
- 1202 Bijma, J., Hönisch, B., and Zeebe, R. E.: Impact of the ocean carbonate chemistry on living
1203 foraminiferal shell weight: Comment on “Carbonate ion concentration in glacial-age deep
1204 waters of the Caribbean Sea” by W. S. Broecker and E. Clark: COMMENT, *Geochem.-*
1205 *Geophys.-Geosyst.*, 3, 1–7, <https://doi.org/10.1029/2002GC000388>, 2002.
- 1206 Bird, C., Darling, K. F., Russell, A. D., Davis, C. V., Fehrenbacher, J., Free, A., Wyman, M.,
1207 and Ngwenya, B. T.: Cyanobacterial endobionts within a major marine planktonic calcifier
1208 (*Globigerina bulloides*, Foraminifera) revealed by 16S rRNA metabarcoding,
1209 *Biogeosciences*, 14, 901–920, <https://doi.org/10.5194/bg-14-901-2017>, 2017.
- 1210 Bollmann, J., Herrle, J. O., Cortés, M. Y., and Fielding, S. R.: The effect of sea water salinity
1211 on the morphology of *Emiliana huxleyi* in plankton and sediment samples, *Earth and*
1212 *Planetary Science Letters*, 284, 320–328, <https://doi.org/10.1016/j.epsl.2009.05.003>, 2009.
- 1213 Burke, J. E., Renema, W., Henehan, M. J., Elder, L. E., Davis, C. V., Maas, A. E., Foster, G.
1214 L., Schiebel, R., and Hull, P. M.: Factors influencing test porosity in planktonic foraminifera,
1215 *Biogeosciences*, 15, 6607–6619, <https://doi.org/10.5194/bg-15-6607-2018>, 2018.

1216 Canals, M., Puig, P., de Madron, X. D., Heussner, S., Palanques, A., and Fabres, J.: Flushing
1217 submarine canyons, *Nature*, 444, 354–357, <https://doi.org/10.1038/nature05271>, 2006.

1218 Chapman, M. R.: Seasonal production patterns of planktonic foraminifera in the NE Atlantic
1219 Ocean: Implications for paleotemperature and hydrographic reconstructions: currents,
1220 *Paleoceanography*, 25, <https://doi.org/10.1029/2008PA001708>, 2010.

1221 Cisneros, M., Cacho, I., Frigola, J., Canals, M., Masqué, P., Martrat, B., Casado, M., Grimalt,
1222 J. O., Pena, L. D., Margaritelli, G., and Lirer, F.: Sea surface temperature variability in the
1223 central-western Mediterranean Sea during the last 2700 years: a multi-proxy and multi-
1224 record approach, *Clim. Past*, 12, 849–869, <https://doi.org/10.5194/cp-12-849-2016>, 2016.

1225 Cléroux, C., Lynch-Stieglitz, J., Schmidt, M. W., Cortijo, E., and Duplessy, J.-C.: Evidence for
1226 calcification depth change of *Globorotalia truncatulinoides* between deglaciation and
1227 Holocene in the Western Atlantic Ocean, *Marine Micropaleontology*, 73, 57–61,
1228 <https://doi.org/10.1016/j.marmicro.2009.07.001>, 2009.

1229 Coppola L., Diamond Riquier E.: MOOSE (DYFAMED), <https://doi.org/10.18142/131>, 2008.

1230 Coppola, L., Raimbault, P., Mortier, L., and Testor, P. Monitoring the environment in the
1231 northwestern Mediterranean Sea, *Eos*, 100, <https://doi.org/10.1029/2019EO125951>, 2019.

1232 Coppola L., Diamond Riquier E. Carval T., Dyfamed observatory
1233 data. <https://doi.org/10.17882/43749>, 2021.

1234 Davis, C. V., Rivest, E. B., Hill, T. M., Gaylord, B., Russell, A. D., and Sanford, E.: Ocean
1235 acidification compromises a planktic calcifier with implications for global carbon cycling, *Sci*
1236 *Rep*, 7, 2225, <https://doi.org/10.1038/s41598-017-01530-9>, 2017.

1237 Dickson, A. G.: Standard potential of the reaction: $\text{AgCl(s)} + \text{iH(g)} = \text{Ag(s)} + \text{HCl(aq)}$, and and
1238 the standard acidity constant of the ion HSO_4^- in synthetic sea water from 273.15 to 318.15
1239 K, *J. Chem. Thermodyn.*, 22, 113–127, 1990.

1240 Dickson, A. G. and Millero, F. J.: A comparison of the equilibrium constants for the dissociation
1241 of carbonic acid in seawater media, *Deep-Sea Res.*, 34, 1733–1743, 1987.

1242 Dolman, A. M., Groeneveld, J., Mollenhauer, G., Ho, S. L., and Laepple, T.: Estimating
1243 Bioturbation From Replicated Small-Sample Radiocarbon Ages, *Paleoceanog and*
1244 *Paleoclimatol*, 36, <https://doi.org/10.1029/2020PA004142>, 2021.

1245 Doney, S. C., Fabry, V. J., Feely, R. A., and Kleypas, J. A.: Ocean Acidification: The other
1246 CO_2 Problem, *Annu. Rev. Mar. Sci.*, 1, 169–192,
1247 <https://doi.org/10.1146/annurev.marine.010908.163834>, 2009.

1248 Durrieu de Madron, X., Zervakis, V., Theocharis, A., and Georgopoulos, D.: Comments on
1249 “Cascades of dense water around the world ocean,” *Progress in Oceanography*, 64, 83–
1250 90, <https://doi.org/10.1016/j.pocean.2004.08.004>, 2005.

1251 Durrieu de Madron, X., Houpert, L., Puig, P., Sanchez-Vidal, A., Testor, P., Bosse, A.,
1252 Estournel, C., Somot, S., Bourrin, F., Bouin, M. N., Beauverger, M., Beguery, L., Calafat,
1253 A., Canals, M., Cassou, C., Coppola, L., Dausse, D., D’Ortenzio, F., Font, J., Heussner, S.,
1254 Kunesch, S., Lefevre, D., Le Goff, H., Martín, J., Mortier, L., Palanques, A., and Raimbault,
1255 P.: Interaction of dense shelf water cascading and open-sea convection in the northwestern
1256 Mediterranean during winter 2012: shelf cascading and open-sea convection, *Geophys.*
1257 *Res. Lett.*, 40, 1379–1385, <https://doi.org/10.1002/grl.50331>, 2013.

1258 Durrieu de Madron, X., Ramondenc, S., Berline, L., Houpert, L., Bosse, A., Martini, S., Guidi,
1259 L., Conan, P., Curtil, C., Delsaut, N., Kunesch, S., Ghiglione, J. F., Marsaleix, P., Pujo-Pay,
1260 M., Séverin, T., Testor, P., Tamburini, C., and the ANTARES collaboration: Deep sediment
1261 resuspension and thick nepheloid layer generation by open-ocean convection: BNL
1262 generation by open-ocean convection, *J. Geophys. Res. Oceans*, 122, 2291–2318,
1263 <https://doi.org/10.1002/2016JC012062>, 2017.

1264 Estrada, M., Marrasé, C., Latasa, M., Berdalet, E., Delgado, M., and Riera, T.: Variability of
1265 deep chlorophyll maximum characteristics in the Northwestern Mediterranean, *Mar. Ecol.*
1266 *Prog. Ser.*, 92, 289–300, <https://doi.org/10.3354/meps092289>, 1993.

1267 Figuerola, B., Hancock, A. M., Bax, N., Cummings, V. J., Downey, R., Griffiths, H. J., Smith,
1268 J., and Stark, J. S.: A Review and Meta-Analysis of Potential Impacts of Ocean Acidification
1269 on Marine Calcifiers From the Southern Ocean, *Front. Mar. Sci.*, 8, 584445,
1270 <https://doi.org/10.3389/fmars.2021.584445>, 2021.

1271 Fox, L., Stukins, S., Hill, T., and Miller, C. G.: Quantifying the Effect of Anthropogenic Climate
1272 Change on Calcifying Plankton, *Sci Rep*, 10, 1620, [https://doi.org/10.1038/s41598-020-](https://doi.org/10.1038/s41598-020-58501-w)
1273 [58501-w](https://doi.org/10.1038/s41598-020-58501-w), 2020.

1274 Hassoun, A. E. R., Gemayel, E., Krasakopoulou, E., Goyet, C., Abboud-Abi Saab, M.,
1275 Guglielmi, V., Touratier, F., and Falco, C.: Acidification of the Mediterranean Sea from
1276 anthropogenic carbon penetration, *Deep Sea Research Part I: Oceanographic Research*
1277 *Papers*, 102, 1–15, <https://doi.org/10.1016/j.dsr.2015.04.005>, 2015.

1278 Hassoun, A. E. R., Bantelman, A., Canu, D., Comeau, S., Galdies, C., Gattuso, J.-P., Giani,
1279 M., Grelaud, M., Hendriks, I. E., Ibello, V., Idrissi, M., Krasakopoulou, E., Shaltout, N.,
1280 Solidoro, C., Swarzenski, P. W., and Ziveri, P.: Ocean acidification research in the
1281 Mediterranean Sea: Status, trends and next steps, *Front. Mar. Sci.*, 9, 892670,
1282 <https://doi.org/10.3389/fmars.2022.892670>, 2022.

1283 Head, M. J., Zalasiewicz, J. A., Waters, C. N., Turner, S. D., Williams, M., Barnosky, A. D.,
1284 Steffen, W., Wagerich, M., Haff, P. K., Syvitski, J., Leinfelder, R., McCarthy, F. M. G., Rose,
1285 N. L., Wing, S. L., An, Z., Cearreta, A., Cundy, A. B., Fairchild, I. J., Han, Y., Sul, J. A. I. do,
1286 Jeandel, C., McNeill, J. R., and Summerhayes, C. P.: The Anthropocene is a prospective
1287 epoch/series, not a geological event, *Episodes*,
1288 <https://doi.org/10.18814/epiugs/2022/022025>, 2022a.

1289 Head, M. J., Steffen, W., Fagerlind, D., Waters, C. N., Poirier, C., Syvitski, J., Zalasiewicz, J.
1290 A., Barnosky, A. D., Cearreta, A., Jeandel, C., Leinfelder, R., McNeill, J. R., Rose, N. L.,
1291 Summerhayes, C., Wagerich, M., and Zinke, J.: The Great Acceleration is real and provides
1292 a quantitative basis for the proposed Anthropocene Series/Epoch, *Episodes*, 45, 359–376,
1293 <https://doi.org/10.18814/epiugs/2021/021031>, 2022b.

1294 Heaton, T. J., Köhler, P., Butzin, M., Bard, E., Reimer, R. W., Austin, W. E. N., Bronk Ramsey,
1295 C., Grootes, P. M., Hughen, K. A., Kromer, B., Reimer, P. J., Adkins, J., Burke, A., Cook,
1296 M. S., Olsen, J., and Skinner, L. C.: Marine20—The Marine Radiocarbon Age Calibration
1297 Curve (0–55,000 cal BP), *Radiocarbon*, 62, 779–820,
1298 <https://doi.org/10.1017/RDC.2020.68>, 2020.

1299 Hemleben, C., Spindler, M., and Anderson, O. R.: *Modern Planktonic Foraminifera*, 1989.

1300 Heussner, S., Durrieu de Madron, X., Calafat, A., Canals, M., Carbonne, J., Delsaut, N., and
1301 Saragoni, G.: Spatial and temporal variability of downward particle fluxes on a continental
1302 slope: Lessons from an 8-yr experiment in the Gulf of Lions (NW Mediterranean), *Marine*
1303 *Geology*, 234, 63–92, <https://doi.org/10.1016/j.margeo.2006.09.003>, 2006.

1304 Houpert, L., Durrieu de Madron, X., Testor, P., Bosse, A., D’Ortenzio, F., Bouin, M. N.,
1305 Dausse, D., Le Goff, H., Kunesch, S., Labaste, M., Coppola, L., Mortier, L., and Raimbault,
1306 P.: Observations of open-ocean deep convection in the northwestern Mediterranean Sea:
1307 Seasonal and interannual variability of mixing and deep water masses for the 2007-2013
1308 Period: deep convection obs. NWMED 2007-2013, *J. Geophys. Res. Oceans*, 121, 8139–
1309 8171, <https://doi.org/10.1002/2016JC011857>, 2016.

1310 IPCC: *The Ocean and Cryosphere in a Changing Climate: Special Report of the*
1311 *Intergovernmental Panel on Climate Change*, 1st ed., Cambridge University Press,
1312 <https://doi.org/10.1017/9781009157964>, 2022.

1313 Jonkers, L., Hillebrand, H., and Kucera, M.: Global change drives modern plankton
1314 communities away from the pre-industrial state, *Nature*, 570, 372–375,
1315 <https://doi.org/10.1038/s41586-019-1230-3>, 2019.

1316 Kiss, P., Jonkers, L., Hudáčková, N., Reuter, R. T., Donner, B., Fischer, G., and Kucera, M.:
1317 Determinants of Planktonic Foraminifera Calcite Flux: Implications for the Prediction of

1318 Intra- and Inter-Annual Pelagic Carbonate Budgets, *Global Biogeochem Cycles*, 35,
1319 <https://doi.org/10.1029/2020GB006748>, 2021.

1320 Kroeker, K. J., Kordas, R. L., Crim, R., Hendriks, I. E., Ramajo, L., Singh, G. S., Duarte, C.
1321 M., and Gattuso, J.: Impacts of ocean acidification on marine organisms: quantifying
1322 sensitivities and interaction with warming, *Glob Change Biol*, 19, 1884–1896,
1323 <https://doi.org/10.1111/gcb.12179>, 2013.

1324 Kuroyanagi, A. and Kawahata, H.: Vertical distribution of living planktonic foraminifera in the
1325 seas around Japan, *Marine Micropaleontology*, 53, 173–196,
1326 <https://doi.org/10.1016/j.marmicro.2004.06.001>, 2004.

1327 LeGrande, A. N., Lynch-Stieglitz, J., and Farmer, E. C.: Oxygen isotopic composition of
1328 *Globorotalia truncatulinoides* as a proxy for intermediate depth density: $\delta^{18}\text{O}$
1329 *Truncatulinoides* as proxy for mid-depth density, *Paleoceanography*, 19, n/a-n/a,
1330 <https://doi.org/10.1029/2004PA001045>, 2004.

1331 Lirer, F., Sprovieri, M., Vallefucio, M., Ferraro, L., Pelosi, N., Giordano, L., and Capotondi, L.:
1332 Planktonic foraminifera as bio-indicators for monitoring the climatic changes that have
1333 occurred over the past 2000 years in the southeastern Tyrrhenian Sea, *Integrative Zoology*,
1334 9, 542–554, <https://doi.org/10.1111/1749-4877.12083>, 2014.

1335 Lohmann, G. P. and Schweitzer, P. N.: *Globorotalia truncatulinoides*' Growth and chemistry
1336 as probes of the past thermocline: 1. Shell size, *Paleoceanography*, 5, 55–75,
1337 <https://doi.org/10.1029/PA005i001p00055>, 1990.

1338 Lombard, F., Erez, J., Michel, E., and Labeyrie, L.: Temperature effect on respiration and
1339 photosynthesis of the symbiont-bearing planktonic foraminifera *Globigerinoides ruber*,
1340 *Orbulina universa*, and *Globigerinella siphonifera*, *Limnol. Oceanogr.*, 54, 210–218,
1341 <https://doi.org/10.4319/lo.2009.54.1.0210>, 2009.

1342 Lombard, F., da Rocha, R. E., Bijma, J., and Gattuso, J.-P.: Effect of carbonate ion
1343 concentration and irradiance on calcification in planktonic foraminifera, *Biogeosciences*, 7,
1344 247–255, <https://doi.org/10.5194/bg-7-247-2010>, 2010.

1345 Lombard, F., Labeyrie, L., Michel, E., Bopp, L., Cortijo, E., Retailleau, S., Howa, H., and
1346 Jorissen, F.: Modelling planktic foraminifer growth and distribution using an
1347 ecophysiological multi-species approach, *Biogeosciences*, 8, 853–873,
1348 <https://doi.org/10.5194/bg-8-853-2011>, 2011.

1349 Loulergue, L., Parrenin, F., and Blunier, T.: New constraints on the gas age-ice age difference
1350 along the EPICA ice cores, 0–50 kyr, *Clim. Past*, 14, 2007.

1351 Lüthi, D., Le Floch, M., Bereiter, B., Blunier, T., Barnola, J.-M., Siegenthaler, U., Raynaud, D.,
1352 Jouzel, J., Fischer, H., Kawamura, K., and Stocker, T. F.: High-resolution carbon dioxide
1353 concentration record 650,000–800,000 years before present, *Nature*, 453, 379–382,
1354 <https://doi.org/10.1038/nature06949>, 2008.

1355 Margaritelli, G.: *Globorotalia truncatulinoides* in Central - Western Mediterranean Sea during
1356 the Little Ice Age, *Marine Micropaleontology*, 11, 2020.

1357 Margaritelli, G., Lirer, F., Schroeder, K., Cloke-Hayes, A., Caruso, A., Capotondi, L., Broggy,
1358 T., Cacho, I., and Sierro, F. J.: *Globorotalia truncatulinoides* in the Mediterranean Basin
1359 during the Middle–Late Holocene: Bio-Chronological and Oceanographic Indicator,
1360 *Geosciences*, 12, 244, <https://doi.org/10.3390/geosciences12060244>, 2022.

1361 Marshall, B. J., Thunell, R. C., Henehan, M. J., Astor, Y., and Wejnert, K. E.: Planktonic
1362 foraminiferal area density as a proxy for carbonate ion concentration: A calibration study
1363 using the Cariaco Basin ocean time series: foraminiferal area density [CO₃²⁻] PROXY,
1364 *Paleoceanography*, 28, 363–376, <https://doi.org/10.1002/palo.20034>, 2013.

1365 Marty, J.-C., Chiavérini, J., Pizay, M.-D., and Avril, B.: Seasonal and interannual dynamics of
1366 nutrients and phytoplankton pigments in the western Mediterranean Sea at the DYFAMED
1367 time-series station (1991–1999), *Deep Sea Research Part II: Topical Studies in*
1368 *Oceanography*, 49, 1965–1985, [https://doi.org/10.1016/S0967-0645\(02\)00022-X](https://doi.org/10.1016/S0967-0645(02)00022-X), 2002.

1369 Mehrbach, C., Culberson, C. H., Hawley, J. E., and Pytkowicz, R. M.: measurement of the
1370 apparent dissociation constants of carbonic acid in seawater at atmospheric pressure,
1371 *Limnol. Oceanogr.*, 18, 897–907, <https://doi.org/10.4319/lo.1973.18.6.0897>, 1973.

1372 Meier, K. J. S., Beaufort, L., Heussner, S., Ziveri, P., and Université, A.-M.: The role of ocean
1373 acidification in *Emiliania huxleyi* coccolith thinning in the Mediterranean Sea, 13, 2014.

1374 Millot, C.: The Gulf of Lions' hydrodynamics, *Continental Shelf Research*, 10, 885–894,
1375 [https://doi.org/10.1016/0278-4343\(90\)90065-T](https://doi.org/10.1016/0278-4343(90)90065-T), 1990.

1376 de Moel, H., Ganssen, G. M., Peeters, F. J. C., Jung, S. J. A., Kroon, D., Brummer, G. J. A.,
1377 and Zeebe, R. E.: Planktic foraminiferal shell thinning in the Arabian Sea due to
1378 anthropogenic ocean acidification?, 9, 2009.

1379 Monaco, A., de Madron, X. D., Radakovitch, O., Heussner, S., and Carbonne, J.: Origin and
1380 variability of downward biogeochemical fluxes on the Rhone continental margin (NW
1381 mediterranean), 29, 1999.

1382 Moy, A. D., Howard, W. R., Bray, S. G., and Trull, T. W.: Reduced calcification in modern
1383 Southern Ocean planktonic foraminifera, *Nature Geosci*, 2, 276–280,
1384 <https://doi.org/10.1038/ngeo460>, 2009.

1385 Nguyen, T. M. P., Petrizzo, M. R., and Speijer, R. P.: Experimental dissolution of a fossil
1386 foraminiferal assemblage (Paleocene–Eocene Thermal Maximum, Dababiya, Egypt):
1387 Implications for paleoenvironmental reconstructions, *Marine Micropaleontology*, 73, 241–
1388 258, <https://doi.org/10.1016/j.marmicro.2009.10.005>, 2009.

1389 Orr, J. C., Fabry, V. J., Aumont, O., Bopp, L., Doney, S. C., Feely, R. A., Gnanadesikan, A.,
1390 Gruber, N., Ishida, A., Joos, F., Key, R. M., Lindsay, K., Maier-Reimer, E., Matear, R.,
1391 Monfray, P., Mouchet, A., Najjar, R. G., Plattner, G.-K., Rodgers, K. B., Sabine, C. L.,
1392 Sarmiento, J. L., Schlitzer, R., Slater, R. D., Totterdell, I. J., Weirig, M.-F., Yamanaka, Y.,
1393 and Yool, A.: Anthropogenic ocean acidification over the twenty-first century and its impact
1394 on calcifying organisms, *Nature*, 437, 681–686, <https://doi.org/10.1038/nature04095>, 2005.

1395 Osborne, E. B., Thunell, R. C., Marshall, B. J., Holm, J. A., Tappa, E. J., Benitez-Nelson, C.,
1396 Cai, W., and Chen, B.: Calcification of the planktonic foraminifera *Globigerina bulloides* and
1397 carbonate ion concentration: Results from the Santa Barbara Basin, *Paleoceanography*,
1398 31, 1083–1102, <https://doi.org/10.1002/2016PA002933>, 2016.

1399 Pallacks, S., Anglada-Ortiz, G., Belen Martrat, P. Graham Mortyn, Grelaud, M., Incarbona, A.,
1400 Schiebel, R., Garcia-Orellana, J., and Ziveri, P.: Western Mediterranean marine cores show
1401 that foraminiferal mass and flux are being influenced by enhanced anthropogenic pressure,
1402 <https://doi.org/10.13140/RG.2.2.26245.99045>, 2020a.

1403 Pallacks, S., Anglada-Ortiz, G., Belen Martrat, P. Graham Mortyn, Grelaud, M., Incarbona, A.,
1404 Schiebel, R., Garcia-Orellana, J., and Ziveri, P.: Western Mediterranean marine cores show
1405 that foraminiferal test calcite mass is being influenced by enhanced anthropogenic
1406 pressure, <https://doi.org/10.13140/RG.2.2.34091.57124>, 2020b.

1407 Parrenin, F., Jouzel, J., Kawamura, K., Lemieux-Dudon, B., Loulergue, L., Masson-Delmotte,
1408 V., Narcisi, B., Raisbeck, G., Raynaud, D., Ruth, U., Schwander, J., Severi, M., Spahni, R.,
1409 Steffensen, J. P., Svensson, A., Udisti, R., Waelbroeck, C., and Wolff, E.: The EDC3
1410 chronology for the EPICA Dome C ice core, *Clim. Past*, 13, 2007.

1411 Pujol, C. and Grazzini, C. V.: Distribution patterns of live planktic foraminifera as related to
1412 regional hydrography and productive systems of the Mediterranean Sea, *Marine*
1413 *Micropaleontology*, 25, 187–217, [https://doi.org/10.1016/0377-8398\(95\)00002-I](https://doi.org/10.1016/0377-8398(95)00002-I), 1995.

1414 Rebotim, A., Voelker, A. H. L., Jonkers, L., Waniek, J. J., Meggers, H., Schiebel, R., Fraile, I.,
1415 Schulz, M., and Kucera, M.: Factors controlling the depth habitat of planktonic foraminifera
1416 in the subtropical eastern North Atlantic, *Biogeosciences*, 14, 827–859,
1417 <https://doi.org/10.5194/bg-14-827-2017>, 2017.

1418 Reimer, P. J. and Reimer, R. W.: A Marine Reservoir Correction Database and On-Line
1419 Interface, *Radiocarbon*, 43, 461–463, <https://doi.org/10.1017/S0033822200038339>, 2001.

- 1420 Rigual-Hernández, A. S., Sierro, F. J., Bárcena, M. A., Flores, J. A., and Heussner, S.:
1421 Seasonal and interannual changes of planktic foraminiferal fluxes in the Gulf of Lions (NW
1422 Mediterranean) and their implications for paleoceanographic studies: Two 12-year
1423 sediment trap records, *Deep Sea Research Part I: Oceanographic Research Papers*, 66,
1424 26–40, <https://doi.org/10.1016/j.dsr.2012.03.011>, 2012.
- 1425 Sabine, C. L., Feely, R. A., Gruber, N., Key, R. M., Lee, K., Bullister, J. L., Wanninkhof, R.,
1426 Wong, C. S., Wallace, D. W. R., Tilbrook, B., Millero, F. J., Peng, T.-H., Kozyr, A., Ono, T.,
1427 and Rios, A. F.: The Oceanic Sink for Anthropogenic CO₂, *Science*, 305, 367–371,
1428 <https://doi.org/10.1126/science.1097403>, 2004.
- 1429 Schiebel, R.: Planktic foraminiferal sedimentation and the marine calcite budget: marine
1430 calcite budget, *Global Biogeochem. Cycles*, 16, 3-1-3–21,
1431 <https://doi.org/10.1029/2001GB001459>, 2002.
- 1432 Schiebel, R., Waniek, J., Bork, M., and Hemleben, C.: Planktic foraminiferal production
1433 stimulated by chlorophyll redistribution and entrainment of nutrients, *Deep Sea Research
1434 Part I: Oceanographic Research Papers*, 48, 721–740, [https://doi.org/10.1016/S0967-
1435 0637\(00\)00065-0](https://doi.org/10.1016/S0967-0637(00)00065-0), 2001.
- 1436 Schiebel, R. and Hemleben, C.: Interannual variability of planktic foraminiferal populations
1437 and test flux in the eastern North Atlantic Ocean (JGOFS), 44, 2000.
- 1438 Schiebel, R. and Hemleben, C.: *Planktic Foraminifers in the Modern Ocean*, Springer Berlin
1439 Heidelberg, Berlin, Heidelberg, <https://doi.org/10.1007/978-3-662-50297-6>, 2017.
- 1440 Schiebel, R. and Hemleben, Ch.: Modern planktic foraminifera, *Palaeont. Z.*, 79, 135–148,
1441 2005.
- 1442 Schiebel, R., Waniek, J., Zeltner, A., and Alves, M.: Impact of the Azores Front on the
1443 distribution of planktic foraminifers, shelled gastropods, and coccolithophorids, *Deep Sea
1444 Research Part II: Topical Studies in Oceanography*, 49, 4035–4050,
1445 [https://doi.org/10.1016/S0967-0645\(02\)00141-8](https://doi.org/10.1016/S0967-0645(02)00141-8), 2002.
- 1446 Schneider, A., Wallace, D. W. R., and Körtzinger, A.: Alkalinity of the Mediterranean Sea:
1447 alkalinity of the mediterranean sea, *Geophys. Res. Lett.*, 34,
1448 <https://doi.org/10.1029/2006GL028842>, 2007.
- 1449 Stuiver, M. and Braziunas, T. F.: Modeling Atmospheric ¹⁴C Influences and ¹⁴C Ages of
1450 Marine Samples to 10,000 BC, *Radiocarbon*, 35, 137–189,
1451 <https://doi.org/10.1017/S0033822200013874>, 1993.
- 1452 Stuiver, M. and Reimer, P. J.: Extended ¹⁴C Data Base and Revised CALIB 3.0 ¹⁴C Age
1453 Calibration Program, *Radiocarbon*, 35, 215–230,
1454 <https://doi.org/10.1017/S0033822200013904>, 1993.
- 1455 Takagi, H., Kimoto, K., Fujiki, T., Saito, H., Schmidt, C., Kucera, M., and Moriya, K.:
1456 Characterizing photosymbiosis in modern planktonic foraminifera, *Biogeosciences*, 16,
1457 3377–3396, <https://doi.org/10.5194/bg-16-3377-2019>, 2019.
- 1458 Touratier, F., Guglielmi, V., Goyet, C., Prieur, L., Pujol-Pay, M., Conan, P., and Falco, C.:
1459 Distributions of the carbonate system properties, anthropogenic CO₂ and acidification
1460 during the 2008 BOUM cruise (Mediterranean Sea), *Biogeochemistry: Open Ocean*,
1461 <https://doi.org/10.5194/bgd-9-2709-2012>, 2012.
- 1462 de Villiers, S.: Optimum growth conditions as opposed to calcite saturation as a control on the
1463 calcification rate and shell-weight of marine foraminifera, *Marine Biology*, 144, 45–49,
1464 <https://doi.org/10.1007/s00227-003-1183-8>, 2004.
- 1465 Weinkauff, M. F. G., Kunze, J. G., Waniek, J. J., and Kučera, M.: Seasonal Variation in Shell
1466 Calcification of Planktonic Foraminifera in the NE Atlantic Reveals Species-Specific
1467 Response to Temperature, Productivity, and Optimum Growth Conditions, *PLoS ONE*, 11,
1468 e0148363, <https://doi.org/10.1371/journal.pone.0148363>, 2016
- 1469 Wilke, I., Meggers, H., and Bickert, T.: Depth habitats and seasonal distributions of recent
1470 planktic foraminifers in the Canary Islands region (29°N) based on oxygen isotopes, *Deep*

1471 Sea Research Part I: Oceanographic Research Papers, 56, 89–106,
1472 <https://doi.org/10.1016/j.dsr.2008.08.001>, 2009.
1473 Zarkogiannis, S. D., Iwasaki, S., Rae, J. W. B., Schmidt, M. W., Mortyn, P. G., Kontakiotis,
1474 G., Hertzberg, J. E., and Rickaby, R. E. M.: Calcification, Dissolution and Test Properties
1475 of Modern Planktonic Foraminifera From the Central Atlantic Ocean, *Front. Mar. Sci.*, 9,
1476 864801, <https://doi.org/10.3389/fmars.2022.864801>, 2022.
1477